

Integrable scattering theories with unstable particles

O.A. Castro-Alvaredo¹, J. Dreißig², A. Fring³

Institut für Theoretische Physik, Freie Universität Berlin, Arnimallee 14, 14195 Berlin, Germany

Received: 24 November 2003 /

Published online: 11 May 2004 – © Springer-Verlag / Società Italiana di Fisica 2004

Abstract. We formulate a new bootstrap principle which allows for the construction of particle spectra involving unstable as well as stable particles. We comment on the general Lie algebraic structure which underlies theories with unstable particles and propose several new scattering matrices. We find a new Lie algebraic decoupling rule, which predicts the renormalization group flow in dependence of the relative ordering of the resonance parameters. The proposals are exemplified for some concrete theories which involve unstable particles, such as the homogeneous sine-Gordon models and their generalizations. The new decoupling rule can be validated by means of our new bootstrap principle and also via the renormalization group flow, which we obtain from a thermodynamic Bethe ansatz analysis.

1 Introduction

One of the central quantities in the study of quantum field theories is the scattering matrix S , which relates asymptotic in and out states. In particular in $1 + 1$ space-time dimensions and when concentrating in addition on integrable theories in this context, the bootstrap principle [1] has turned out to be a very powerful non-perturbative construction tool. Many consistent exact scattering matrices have been determined based on this idea. Exact is here always to be understood in the sense that S is known to all orders in perturbation theory. The bootstrap principle was also successfully generalized to theories in half-space [2], theories with purely transmitting defects [3] and even theories which possess infinitely many resonance states [4]. However, hitherto there exists no formulation of a construction principle leading to unstable particles in the spectrum. Some specific theories containing unstable particles are known, but so far the latter emerge as poles in the unphysical sheet as by-products in the scattering process of two stable particles. A description of the scattering process of an unstable particle with another stable or unstable particle is entirely missing in this context. Obviously, scattering processes involving unstable particles do occur in nature, such that the quest for a proper prescription is of physical relevance. It is also clear that this cannot be a scattering theory in the usual sense, since for that

one requires the particles involved to exist asymptotically, i.e. for $t \rightarrow \infty$. Clearly any unstable particle will vanish in this limit rendering such a formulation meaningless at first sight. Nonetheless, some particles have extremely long lifetimes, and appear to exist quasi-infinitely long from an experimentalist's point of view. It appears therefore natural to seek a principle closely related to the conventional bootstrap for stable particles. One of the main purposes of this paper is to provide such a construction principle.

Our bootstrap proposal has the following predictive power.

- (a) It yields the amount of unstable particles together with their mass. This prediction can be used to explain a mass degeneracy of some unstable particles which cannot be seen in a thermodynamic Bethe ansatz (TBA) analysis.
- (b) It yields the three-point couplings of all possible interactions, that is, involving stable as well as unstable particles.
- (c) It is in agreement with a general Lie algebraic decoupling rule, which we also propose in this paper, describing the behavior when certain resonance parameters tend to infinity.

We illustrate the working of the bootstrap for some concrete theories which are known to contain unstable particles in their spectrum, the homogeneous sine-Gordon models (HSG) [5]. For these models we also test the newly proposed decoupling rule, which predicts the renormalization group (RG) flow from the ultraviolet to the infrared directly on the level of the scattering matrix constructed from the new bootstrap principle and also by means of a TBA analysis.

2 A bootstrap for unstable particles

In general unstable particles of finite life time τ are described by complexifying the physical mass of a stable particle, by adding a decay width $\Gamma \sim \hbar/\tau$. This prescription

Present addresses:

¹ Laboratoire de Physique, Ecole Normale Supérieure de Lyon, Allée d'Italie, 69364 Lyon Cedex, France, e-mail: ocastroa@ens-lyon.fr

² Universität Potsdam, Institut für Physik, Am Neuen Palais 10, 14469 Potsdam, Germany, e-mail: julian.dreissig@qipc.org

³ Centre for Mathematical Science, City University, Northampton Square, London EC1V 0HB, UK, e-mail: A.Fring@city.ac.uk

is well established in quantum mechanics, see e.g. [6], and can also be applied similarly in the quantum field theory context; see e.g. [7]. When describing the latter by means of a scattering theory, the formation of an unstable particle (ij) from two stable ones of type i and j is well understood. In that case the creation process is reflected by a pole in the scattering matrix S_{ij} as a function of the Mandelstam variable at $s_{ij} = (m_{(ij)} - i\Gamma_{(ij)}/2)^2$. As discussed for instance in [7], whenever $m_{(ij)} \gg \Gamma_{(ij)}$, the quantity $m_{(ij)}$ admits a clear cut interpretation as the physical mass. Transforming as usual in this context from the Mandelstam variable s to the rapidity variable θ and describing the scattering of the two stable particles of type i and j with masses m_i and m_j by an S-matrix $S_{ij}(\theta)$, the resonance pole is situated at $\eta_{ij}^{(ij)} = \gamma_{ij}^{(ij)} - i\bar{\gamma}_{ij}^{(ij)}$ with resonance parameters $\gamma_{ij}^{(ij)}, \bar{\gamma}_{ij}^{(ij)} \in \mathbb{R}^+$. It is crucial to note that the formation of the unstable particle is accompanied by parity breaking, and poles with $\gamma_{ij}^{(ij)} \in \mathbb{R}^-$ are not associated to such a process. Identifying the real and imaginary parts of the pole yields the well-known Breit–Wigner equations [8]

$$m_{(ij)}^2 - \frac{\Gamma_{ij}^2}{4} = m_i^2 + m_j^2 + 2m_i m_j \cosh \gamma_{ij}^{(ij)} \cos \bar{\gamma}_{ij}^{(ij)}, \tag{2.1}$$

$$m_{(ij)} \Gamma_{ij} = 2m_i m_j \sinh \gamma_{ij}^{(ij)} \sin \bar{\gamma}_{ij}^{(ij)}. \tag{2.2}$$

Eliminating the decay width from (2.1) and (2.2), we can express the mass of the unstable particles $m_{(ij)}$ in the model as a function of the masses of the stable particles m_i, m_j and the resonance parameter $\gamma_{ij}^{(ij)}$. A simple consequence of (2.1) and (2.2) is that for large resonance parameters $\gamma_{ij}^{(ij)}$ the masses of the unstable particles are

$$m_{(ij)} \sim \sqrt{m_i m_j} e^{\gamma_{ij}^{(ij)}/2}, \tag{2.3}$$

which is a relation we will appeal to quite frequently. In some places of the literature, e.g. [10, 11], the absolute value of $\gamma_{ij}^{(ij)}$ is used in (2.2) rather than $\gamma_{ij}^{(ij)}$ itself, which seems to suggest that the sign of $\gamma_{ij}^{(ij)}$ is not relevant. This contradicts, however, the findings of the thermodynamic Bethe ansatz (TBA) analysis below, in which the signs turn out to be crucial, and we want to argue here that in fact this absolute value is not needed and even leads to wrong predictions if implemented. To manifest this point of view, let us first look at a heuristic argument and consider the two-particle wave functions $\psi_{ij} \sim \exp(-\Gamma_{ij} t)$ and $\psi_{ji} \sim \exp(-\Gamma_{ji} t)$ associated to the scattering of particles i with j and vice versa. When choosing for definiteness $\Gamma_{ij} > 0$, the function ψ_{ij} decays for $t \rightarrow \infty$ and ψ_{ji} decays for $t \rightarrow -\infty$. This is the effect of parity breaking, suggesting that the unstable particle (\bar{ij}) is formed in the process

$$i + j \rightarrow (\bar{ij}) \tag{2.4}$$

rather than $j + i$. As common also for stable particles we distinguish the anti-particle of an unstable particle by an overbar, i.e. (\bar{ij}) is the anti-particle of (ij) . In general in our notation the unstable particles can be recognized

as they carry the names of their parents, where the two names are inherited. This interpretation is compatible with a PT -transformation and hence no absolute value is needed in (2.2). A reason for an artificial introduction of an absolute value is that apparently in (2.2) the parameter Γ can become negative for $\gamma_{ij}^{(ij)} < 0$, which is unphysical. However, once one also attaches indices to the decay width, this concern is eliminated and one obtains a clear physical meaning for these values. A less heuristic validation of this point of view will be obtained from our TBA analysis presented in Sect. 4.2.

One may now ask the natural question whether one can cross the unstable particle to the other side in the process (2.4), that is: do the processes $(ij) + i$ or $j + (ij)$ make any sense and, furthermore, is it possible to formulate a bootstrap principle for unstable particles? To formulate such a principle is highly desirable, since it would allow for an explicit construction of unstable particles. Up to now they only emerge indirectly, somewhat as a side product once the stable particle content has been determined.

As already mentioned in the introduction, the main conceptual obstacle in the formulation of a bootstrap principle for unstable particles is the fact that in a well-defined scattering theory one always deals with asymptotic states. Nonetheless, one may seek an approach closely related to a properly defined S-matrix.

Let us formulate the bootstrap principle: We commence with the fusing of two stable particles to create an unstable particle as in the process (2.4). To the process (2.4) we can associate bootstrap equations almost in the usual way. We scatter for this with an additional particle, say of type l , and exploit the integrability of the theory. Accordingly the ordering of the scattering is associative, such that we can equate the two situations of either l scattering before or after the creation of the unstable particle. The object which describes the latter process we refer to as $\tilde{S}_{l(ij)}$, indicating with the tilde that we do not view this object as a standard S-matrix since it involves one particle which is unstable. In the conventional formulation one generally assumes that also the created particle exists asymptotically. It is this assumption we propose to relax. We depict the bootstrap equation in Fig. 1. Identifying in Fig. 1 the particle k with (ij) we obtain, according to the outlined

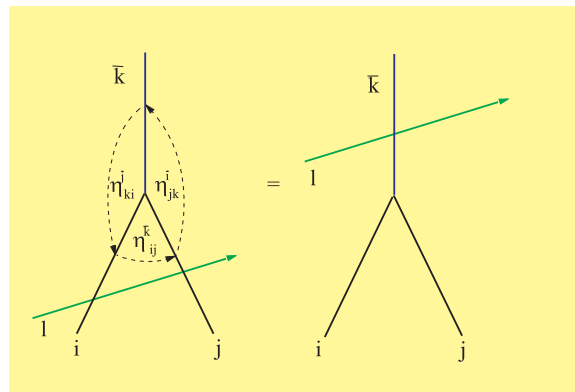


Fig. 1. The bootstrap equations

conventions, the \tilde{S} bootstrap equations

$$\tilde{S}_{li}(\theta - \bar{\eta}_{(ij)i}^{\bar{j}}) \tilde{S}_{lj}(\theta + \bar{\eta}_{j(ij)}^{\bar{j}}) = \tilde{S}_{l(\bar{i}\bar{j})}(\theta), \quad (2.5)$$

where $\bar{\eta} = \pm i\pi - \eta$ and also $\bar{\eta} \rightarrow -\bar{\eta}$ is not a symmetry. In Fig. 1 we indicate that the angles should be measured anti-clockwise, which explains the signs. We also note that we do not assume parity invariance, so that in general $\bar{\eta}_{ji}^{(\bar{i}\bar{j})} \neq \bar{\eta}_{ij}^{(\bar{i}\bar{j})}$. As further analogy between \tilde{S} and S , we assume that the crossing and analyticity relations are maintained:

$$\tilde{S}_{kl}(\theta) = \tilde{S}_{\bar{l}\bar{k}}(i\pi - \theta) \quad \text{and} \quad \tilde{S}_{kl}(\theta) \tilde{S}_{lk}(-\theta) = 1. \quad (2.6)$$

However, we do not demand \tilde{S} to be unitary, for reasons we will comment upon further below. With the help of (2.6), one derives the bootstrap equations for the opposite parity and the ones for the crossed processes $i + (ij) \rightarrow \bar{j}$ and $j + (ij) \rightarrow \bar{i}$ from (2.5)

$$\tilde{S}_{(\bar{i}\bar{j})l}(\theta) = \tilde{S}_{il}(\theta + \bar{\eta}_{(ij)i}^{\bar{j}}) \tilde{S}_{jl}(\theta - \bar{\eta}_{j(ij)}^{\bar{j}}), \quad (2.7)$$

$$\begin{aligned} \tilde{S}_{l\bar{j}}(\theta) &= \tilde{S}_{l(ij)}(\theta - \bar{\eta}_{j(ij)}^{\bar{j}}) \\ &\quad \times \tilde{S}_{li}(\theta \pm i\pi - \bar{\eta}_{(ij)i}^{\bar{j}} - \bar{\eta}_{j(ij)}^{\bar{j}}), \end{aligned} \quad (2.8)$$

$$\begin{aligned} \tilde{S}_{l\bar{i}}(\theta) &= \tilde{S}_{l(ij)}(\theta + \bar{\eta}_{(ij)i}^{\bar{j}}) \\ &\quad \times \tilde{S}_{lj}(\theta \pm i\pi + \bar{\eta}_{(ij)i}^{\bar{j}} + \bar{\eta}_{j(ij)}^{\bar{j}}). \end{aligned} \quad (2.9)$$

From the crossing relation for the scattering matrix and (2.8) or (2.9) one obtains some relations between the various fusing angles:

$$\bar{\eta}_{ij}^{(\bar{i}\bar{j})} + \bar{\eta}_{(ij)i}^{\bar{j}} + \bar{\eta}_{j(ij)}^{\bar{j}} = \pm i\pi. \quad (2.10)$$

At first sight this looks very much like the usual bootstrap prescription, but there are some differences. As is clear from the scattering process of two stable particles producing an unstable one, the angle $\bar{\eta}_{ij}^{(\bar{i}\bar{j})}$ is not purely complex any longer as it is for the situation when exclusively stable particles scatter. As a consequence, this property then extends to the other angles $\bar{\eta}_{(ij)i}^{\bar{j}}$ and $\bar{\eta}_{j(ij)}^{\bar{j}}$ in (2.5), which also possess some non-vanishing real parts. Note that (2.10) implies that the real parts of the three angles involved add up to zero. At this point we do not have an entirely compelling reason for demanding that, but this formulation will turn out to work well. The main conceptual difference is of course that we allow unstable particles to be involved in the scattering processes. In the time interval $0 < t < \tau_{(ij)}$ we could formally associate to those particles some operators $\tilde{Z}_{(ij)}^{\dagger}(\theta)$, with $\lim_{t \rightarrow \infty} \tilde{Z}_{(ij)}^{\dagger}(\theta) = 1$ if $\tau_{(ij)} < \infty$. It is important to note that these operators do not exist asymptotically, such that in general $\langle \tilde{Z}_{(ij)}(\theta) \tilde{Z}_{(ij)}^{\dagger}(\theta') \rangle \neq \delta(\theta - \theta')$. In fact the entire operation of crossing $\tilde{Z}_{(ij)}^{\dagger}(\theta)$ from an in to an out state is ill defined. This property is then reflected in the non-unitarity of \tilde{S} . The loss of unitarity is somewhat natural, since it usually reflects conservation of probabilities, which of course we do not expect in the case of unstable particles.

It can already be anticipated that our proposal will lead to the construction of further unstable particles besides the primary (fundamental) ones created in the scattering process of two stable ones. In the following we shall refer to unstable particles formed in a scattering process involving at least one primary unstable particle as “secondaries” and to those which have at least one secondary as their parent as “tertiaries”, etc. An important observation will be that tertiary particles can be degenerate in mass to stables, primaries or secondaries.

3 Generalities on theories with unstable particles

At present all known theories with unstable particles in their spectrum can be thought of in terms of a simple universal Lie algebraic structure. The formulation is based on an arbitrary simply laced Lie algebra $\tilde{\mathfrak{g}}$ (possibly with a subalgebra \mathfrak{h}) with rank $\tilde{\ell}$ together with its associated Dynkin diagram (for more details see for instance [9]). To each node one attaches a simply laced Lie algebra \mathfrak{g}_i and to each link between the nodes i and j a resonance parameter σ_{ij} , as depicted in the $\mathfrak{g}/\mathfrak{h}$ -coset Dynkin diagram



Besides the usual rules for Dynkin diagrams, we adopt here the convention that we add an arrow to the link, which manifests the parity breaking and allows one to identify the signs of the resonance parameters. An arrow pointing from the node i to j simply indicates that $\sigma_{ij} > 0$. Since, except in Sect. 4.2.6, we are dealing mostly with simply laced Lie algebras, this should not lead to confusion.

As particular examples one can choose for instance $\tilde{\mathfrak{g}}$ to be simply laced and $\mathfrak{g}_1 = \dots = \mathfrak{g}_{\tilde{\ell}} = SU(k)$, in which case one obtains the $\tilde{\mathfrak{g}}_k$ -homogeneous sine-Gordon models [5, 10]. This is generalized [12] when taking instead $\tilde{\mathfrak{g}}$ to be non-simply laced and $\mathfrak{g}_i = SU(2k/\alpha_i^2)$, with α_i being the simple roots of $\tilde{\mathfrak{g}}$. The choice $\mathfrak{g}_1 = \dots = \mathfrak{g}_{\tilde{\ell}} = \mathfrak{g}$ with \mathfrak{g} being any arbitrary simply laced Lie algebra gives the $\mathfrak{g}|\tilde{\mathfrak{g}}$ theories [13]. An example for a theory associated to a coset is the roaming sinh-Gordon model [14], which can be thought of as $\tilde{\mathfrak{g}}/\mathfrak{h} \equiv \lim_{k \rightarrow \infty} SU(k+1)/SU(k)$ with $\mathfrak{g}_1 = \dots = \mathfrak{g}_{\tilde{\ell}} = SU(2)$. It is clear that the examples presented here do not exhaust yet all possible combinations and the structure mentioned above allows for more combinations of algebras, which are not yet explored. One is also not limited to Dynkin diagrams and may consider more general graphs which have multiple links, i.e. resonance parameters, between various nodes. Examples for such theories were proposed and studied in [4].

On the base of this Lie algebraic picture one can then easily construct the scattering matrix. For this, we characterize each particle by two quantum numbers (a, i) , which take their values in different ranges $1 \leq a \leq \ell_i$, where ℓ_i is not necessarily rank \mathfrak{g}_i and $1 \leq i \leq \tilde{\ell} = \text{rank} \tilde{\mathfrak{g}}$. This means

that in total we have $(\tilde{\ell} \times \sum_i \ell_i)$ different particle types. The scattering matrix describing the interaction between these types of particles is then of the general form

$$S_{ab}^{ij}(\theta, \sigma_{ij}) = [S_{ab}^{\min}(\theta)]^{\delta_{ij}} [S_{ab}^{ij}(\theta, \sigma_{ij})]^{\tilde{I}_{ij}}, \quad (3.1)$$

where $S_{ab}^{\min}(\theta)$ corresponds to some scaling model of a statistical model and \tilde{I} is the incidence matrix of $\tilde{\mathfrak{g}}$. It is known that all S-matrices of these scaling models can be viewed as minimal parts of some affine Toda field theory (ATFT) S-matrix [15]. Then $S_{ab}^{ij}(\theta, \sigma_{ij})$ is essentially a CDD factor [16] for which the coupling constant is chosen to be a function of the values i, j . At present, all known scattering theories which involve unstable particles are of this generic form and in particular all of the above mentioned examples.

We propose here yet a further class of scattering matrices. The presented picture makes it very suggestive to be generalized by introducing a coupling constant dependence into such models simply by replacing $S_{ab}^{\min}(\theta)$ by a full affine Toda field theory scattering matrix

$$S_{ab}^{ij}(\theta, B, \sigma_{ij}) := [S_{ab}^{\text{ATFT}}(\theta, B)]^{\delta_{ij}} [S_{ab}^{ij}(\theta, \sigma_{ij})]^{\tilde{I}_{ij}}. \quad (3.2)$$

Obviously this will not alter any of the bootstrap consistency equations, since the difference between the theory with a minimal S-matrix and the one with a coupling constant dependence such as (3.2) is simply a CDD factor. It should also be clear that we may introduce an additional coupling constant into the second factor in (3.2) by a similar consideration. As an illustration of the construction principle (3.2) we present here a new scattering matrix which corresponds to the coupling constant dependent version of the $SU(3)_2$ -HSG model. The two self-conjugate particles in the model named by “+” and “-” interact as

$$S_{\pm\pm}(\theta, B) = \frac{\tanh \frac{1}{2}(\theta - i\frac{\pi}{2}B)}{\tanh \frac{1}{2}(\theta + i\frac{\pi}{2}B)}$$

and

$$S_{\pm\mp}(\theta, \sigma) = \pm \tanh \frac{1}{2}(\theta \pm \sigma - i\frac{\pi}{2}). \quad (3.3)$$

It is easy to check that these matrices satisfy the unitarity-analyticity and crossing relations. There is no pole in the physical sheet, so that no fusing takes place in this model. There exist various distinct limits: Taking the coupling constant B to be real and $0 \leq B \leq 2$ the scattering of two particles of the same type is described by the sinh-Gordon scattering matrix. The analytic continuation $B \rightarrow 1 + i\bar{\sigma}/\pi$ turns $S_{\pm\pm}(\theta)$ into two copies of the roaming trajectory S-matrix of Zamolodchikov [14]. Taking the limit $\bar{\sigma} \rightarrow \infty$ reduces the whole system (3.3) to the usual $SU(3)_2$ -HSG model. The limit $\sigma \rightarrow \infty$ decouples the system into a direct product of two theories described either by the sinh-Gordon scattering matrix, two roaming trajectory S-matrices, two thermally perturbed Ising models or a free boson, depending on the value of B .

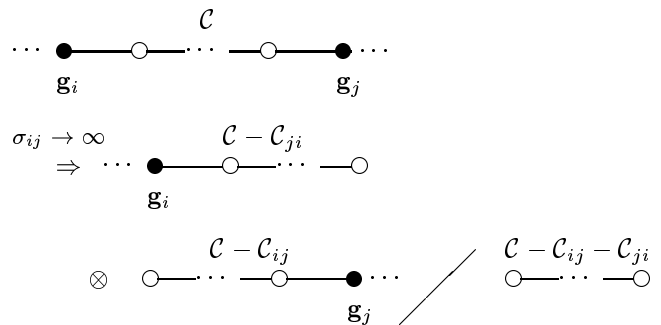
3.1 Decoupling rule

It is of special interest to investigate the behavior of such systems when certain resonance parameters σ_{ij} tend to infinity. According to (2.3) this limit corresponds to a situation when the energy scale of the unstable particle is so large that it can never be created. As a consequence, the particle content of the theory will be altered when such a limit is carried out. This feature should be captured by the bootstrap construction. When taking several of such limits in a consecutive order, this behavior is reflected in addition in the renormalization group flow in the form of the typical staircase pattern of the Virasoro central charge as a function of the inverse temperature as will be discussed below. In the direction from the infrared to the ultraviolet, the flow from one plateau to the next is then associated to the formation of an unstable particle with mass (2.3). The challenge is of course to predict the positions, that is, the height and the on-set of the plateaus, as a function of the temperature. The on-set is simply determined by the formula (2.3). In order to predict the height, i.e. the fixed points of the RG flow, we propose the following.

Decoupling rule: Call the overall Dynkin diagram \mathcal{C} and denote the associated Lie group and Lie algebra by $\tilde{G}_{\mathcal{C}}$ and $\tilde{\mathfrak{g}}_{\mathcal{C}}$, respectively. Let σ_{ij} be some resonance parameter related to the link between the nodes i and j . To each node i attach a simply laced Lie algebra \mathfrak{g}_i . Produce a reduced diagram \mathcal{C}_{ji} containing the node j by cutting the link adjacent to it in the direction i . Likewise produce a reduced diagram \mathcal{C}_{ij} containing the node i by cutting the link adjacent to it in the direction j . Then the $\tilde{G}_{\mathcal{C}}$ -theory decouples according to the rule

$$\lim_{\sigma_{ij} \rightarrow \infty} \tilde{G}_{\mathcal{C}} = \tilde{G}_{(\mathcal{C}-\mathcal{C}_{ij})} \otimes \tilde{G}_{(\mathcal{C}-\mathcal{C}_{ji})} / \tilde{G}_{(\mathcal{C}-\mathcal{C}_{ij}-\mathcal{C}_{ji})}. \quad (3.4)$$

We depict this rule also graphically in terms of Dynkin diagrams:



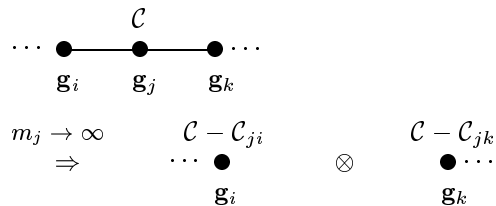
According to the GKO-coset construction [19], this means that the Virasoro central charge flows as

$$c_{\tilde{\mathfrak{g}}_{\mathcal{C}}} \rightarrow c_{\tilde{\mathfrak{g}}_{\mathcal{C}-\mathcal{C}_{ij}}} + c_{\tilde{\mathfrak{g}}_{\mathcal{C}-\mathcal{C}_{ji}}} - c_{\tilde{\mathfrak{g}}_{\mathcal{C}-\mathcal{C}_{ij}-\mathcal{C}_{ji}}}. \quad (3.5)$$

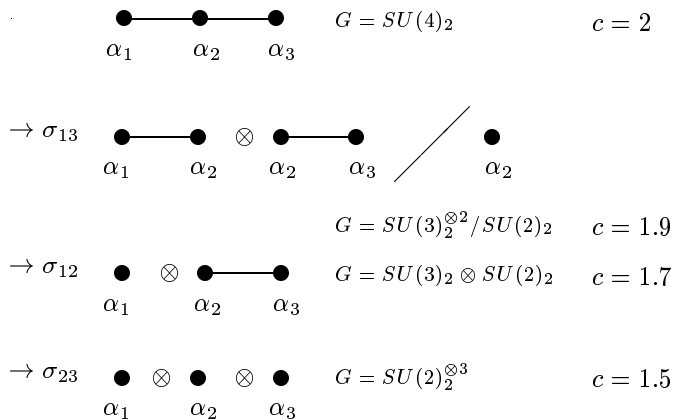
The rule may be applied consecutively to each disconnected subgraph produced according to the decoupling rule. We stress that this rule is really a decoupling rule and not a fusing rule, it only predicts the flow from the ultraviolet to the infrared and not vice versa. This is of course natural, as scaling functions measure the degrees of freedom

of the system and the information loss in the RG flow is irreversible. Hence, potentially we have for the visible unstable particles $[\ell(\ell - 1)/2]!$ different types of flows corresponding to the possible orderings for the masses. For $SU(\ell + 1)$ the particular ordering $\sigma_{2i, 2i+1} > 0, \sigma_{2i-1, 2i} < 0$ with $|\sigma_{2i, 2i+1}| < |\sigma_{2i-1, 2i}|$ leads to the decoupling rule as discussed in [20], which is a special case of (3.4). In the following we shall confirm the general rule (3.4) directly on the level of the scattering matrix and also by means of a TBA analysis which yields the RG flow passing along the central charges as predicted by (3.5).

More familiar is a decoupling rule found by Dynkin [17] for the construction of semi-simple¹ subalgebras $\tilde{\mathfrak{h}}$ from a given algebra $\tilde{\mathfrak{g}}$. For the more general diagrams which can be related to the $\tilde{\mathfrak{g}}_k$ -HSG models the generalized rule can be found in [18]. These rules are all based on removing some of the nodes rather than links. For our physical situation at hand this corresponds to sending all stable particles which are associated to the algebra of a particular node to infinity. As in the decoupling rule (3.4) the number of stable particles remains preserved, it is evident that the two rules are inequivalent. Letting for instance the mass scale in \mathfrak{g}_j go to infinity, the generalized (in the sense that \mathfrak{g}_j can be different from A_ℓ) rule of Kuniba is simply depicted as

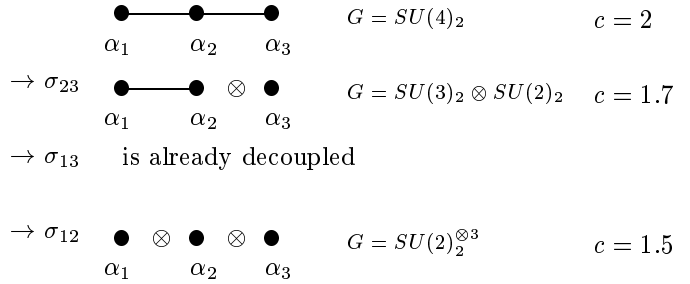


We illustrate the working of the rule (3.4) with the simple example of the $SU(4)_2$ -HSG model. For level 2, we can associate the simple roots to the nodes of the $\tilde{\mathfrak{g}}$ -Dynkin diagram. For the ordering $\sigma_{13} > \sigma_{12} > \sigma_{23}$ we predict from (3.4) the flow



¹ The subalgebras constructed in this way are not necessarily maximal and regular. A guarantee for obtaining those, except in six special cases, is only given when one adequately manipulates the extended Dynkin diagram.

Taking instead the ordering $\sigma_{23} > \sigma_{13} > \sigma_{12}$, we compute



The central charges can be obtained from (4.2) using (3.5). We will elaborate more on this example in Sects. 4.1.2 and 4.2.1 from the bootstrap and TBA point of view, respectively. It is important to note the non-commutative nature of the limiting procedures. For more complicated algebras it is essential to keep track of the labels on the nodes, since only in this way one can decide whether they cancel against the subgroup diagrams or not. See Sect. 4.2 for more details and examples.

4 The homogeneous sine-Gordon models

Let us now consider some specific choice of algebras: $\mathfrak{g}_1 = \dots = \mathfrak{g}_\ell = SU(k)$, which as we mentioned corresponds to the $\tilde{\mathfrak{g}}_k$ -HSG models. These theories have recently attracted some attention, because it could be argued even from a Lagrangian point of view that besides stable particles they also contain unstable particles in their spectrum [5]. The HSG models belong to the huge class of massive integrable models which can be obtained as relevant perturbations from conformal field theories in the spirit of [21]

$$\mathcal{H}_{G_k\text{-HSG}} = \mathcal{H}_{G_k/U(1)^\ell\text{-CFT}} - \lambda \int d^2x \phi(x, t). \quad (4.1)$$

The underlying conformal field theory is a WZNW- $G_k/U(1)^\ell$ -coset theory [19, 22] with k being the level and ℓ the rank of a semi-simple Lie algebra \mathfrak{g} . The Virasoro central charge c and the conformal dimensions $\Delta, \bar{\Delta}$ of the perturbing operator ϕ are

$$c = \ell \frac{k h - h^\vee}{k + h^\vee} \quad \text{and} \quad \Delta = \bar{\Delta} = \frac{h^\vee}{k + h^\vee}. \quad (4.2)$$

Here $(h^\vee)h$ is the (dual) Coxeter number of \mathfrak{g} . In the notation of the massive theory we will not carry along the subalgebra $U(1)^\ell$ as indicated in (4.1) for simplicity. The S-matrices involving the stable particles for simply laced and non-simply laced algebras were proposed in [10] and [12], respectively. Examples on which we will focus a lot in the following are models with level $k = 2$. Adopting the notation of [20], the related scattering matrix may be written for the simply laced case as

$$S_{ij}(\theta, \sigma_{ij}) = (-1)^{\delta_{ij}} \varepsilon(\sigma_{ij})(\sigma_{ij}, 2)^{I_{ij}}, \quad 1 \leq i, j \leq \ell, \quad (4.3)$$

where I denotes the incidence matrix of \mathbf{g} . It is convenient to abbreviate

$$(\sigma, x) := \tanh(\theta + \sigma - i\pi x/4). \tag{4.4}$$

The $\varepsilon(x)$ is the step-function, i.e. $\varepsilon(x) = 1$ for $x \geq 0$, $\varepsilon(x) = -1$ for $x < 0$. The model contains $(\ell - 1)$ linear independent resonance parameters σ_{ij} . As a convenient basis one usually chooses those which can be associated directly to the links in the Dynkin diagram, i.e. the primary unstable particles. The σ 's can be thought of as being composed as a difference $\sigma_{ij} = \sigma_i - \sigma_j$, such that $\sigma_{ij} = -\sigma_{ji}$ and $\sigma_{ij} = \sigma_{ik} + \sigma_{kj}$. Up to now, the precise correspondence between the unstable particles occurring in the HSG model and all these resonance parameters has not been worked out in the literature. So far stable particles were associated to simple roots and unstable particles have been identified on the quantum level as the sum of two simple roots α_i, α_j with $I_{ij} \neq 0$. However, these are only the primaries and as we already mentioned, we also expect to find secondaries, tertiaries, etc. Here we want to provide evidence that unstable particles can in fact be related to *each* non-simple positive root, such that the amount of unstable particles is in fact

$$\# \text{ of unstable particles} = \ell(h - 2)/2. \tag{4.5}$$

It will turn out that not all of these particles are visible in the RG scaling function, since our bootstrap proposal will show that by construction several of the unstable particles are unavoidably degenerate in the mass given by (2.3), such that only $\ell(\ell - 1)/2$ unstable particles will be detectable by a TBA analysis. This means whenever $h = \ell + 1$, as in $SU(\ell + 1)$, we can see all unstable particles in an RG flow, but otherwise not as for instance in $SO(2\ell)$.

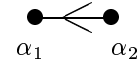
4.1 Bootstrap construction

We present now three examples which we consider to be instructive to illustrate the working of the bootstrap principle as they gradually include new features. The $SU(3)_2$ -HSG model contains only primary unstables, the $SU(4)_2$ model contains in addition secondaries and the $SO(8)_2$ model is an example for a theory with tertiaries and mass degeneracy. Note that for level 2 all particles are self-conjugate.

4.1.1 The $SU(3)_2$ -HSG model

Starting now with the known part of the scattering matrix (4.3) for the stable particles, and leaving the remaining entries which involve unstable particles unknown, we construct consistent solutions to the bootstrap equations (2.5), (2.8), and (2.9). We can fix the imaginary parts of the fusing angles by the requirement that for vanishing resonance parameters we want to reproduce the masses predicted by the Breit–Wigner formula. Choosing the masses of the stable particles to be $m_1 = m_2 = m$ the one for the unstable results in $m_{(12)} = \sqrt{2}m$. This argument does not constrain

the real parts of the fusing angles, so that they are not completely fixed and still contain a certain ambiguity. The different choices of these parameters give rise to slightly different theories. First we consider the case $\sigma_{21} > 0$:



For the $SU(3)_2$ -HSG model with this choice of the resonance parameter, we then find the following bootstrap equations:

$$\begin{aligned} \tilde{S}_{l(12)}(\theta) &= \tilde{S}_{l1}(\theta + (1 - \nu)\sigma_{12} \\ &+ i\pi/4)\tilde{S}_{l2}(\theta - \nu\sigma_{12} - i\pi/4) \end{aligned} \tag{4.6}$$

from which we construct

$$\begin{aligned} \tilde{S}_{SU(3)}(\theta, \sigma_{12}) &= \\ &\begin{pmatrix} -1 & -(\sigma_{12}, 2) & -((1 - \nu)\sigma_{12}, 3) \\ (\sigma_{21}, 2) & -1 & -(\nu\sigma_{21}, 1) \\ -((\nu - 1)\sigma_{12}, 1) & -(\nu\sigma_{12}, 3) & -1 \end{pmatrix}. \end{aligned} \tag{4.7}$$

Here we label the rows and columns in the order $\{1, 2, (12)\}$. According to the principles outlined above, the S-matrix (4.7) allows for the processes

$$1 + 2 \rightarrow (12), \quad 2 + (12) \rightarrow 1, \quad (12) + 1 \rightarrow 2. \tag{4.8}$$

The related fusing angles are read off from (4.7) as

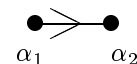
$$\begin{aligned} \eta_{12}^{(12)} &= -i\pi/2 + \sigma_{21}, \\ \eta_{(12)1}^2 &= -3i\pi/4 + (1 - \nu)\sigma_{12}, \\ \eta_{2(12)}^1 &= -3i\pi/4 + \nu\sigma_{12} \end{aligned} \tag{4.9}$$

and are interrelated through (2.10), which still holds even though the η 's have non-vanishing real parts. We can employ these fusing angles and compute the masses and decay widths by means of the Breit–Wigner formulae (2.1) and (2.2). Taking again for simplicity $m_1 = m_2 = m$ and in addition $\nu = 1/2$, we obtain for the first process in (4.8)

$$m_{(12)} = \sqrt{2}m \cosh \sigma_{21}/2 \text{ and } \Gamma_{(12)} = 2\sqrt{2}m \sinh \sigma_{21}/2. \tag{4.10}$$

Employing now also in the process $2 + (12) \rightarrow 1$ the Breit–Wigner formula, we construct in the limit $\sigma_{12} \rightarrow 0$ the values $m_1 = m$ and $\Gamma_1 = 0$. Likewise, in the last process in (4.8) we obtain $m_2 = m$ and $\Gamma_2 = 0$.

The asymptotic limit $t \rightarrow \infty$ becomes meaningful when we operate on an energy scale at which the unstable particle has not even been created yet, i.e. $\Gamma_{(12)} \rightarrow \infty \equiv \sigma_{21} \rightarrow \infty$. In that case the theory decouples into two $SU(2)_2$ models, i.e. free fermions, with $S_{11} = S_{22} = -1$. This is a simple version of the decoupling rule (3.4). We consider now a different theory with $\sigma_{12} > 0$:



Taking now also in this case for simplicity $\nu = 1/2$, we find the following bootstrap satisfied:

$$\tilde{S}_{l(12)}(\theta) = \tilde{S}_{l2}(\theta - \sigma_{12}/2 + i\pi/4)\tilde{S}_{l1}(\theta + \sigma_{12}/2 - i\pi/4), \tag{4.11}$$

which yields the S-matrix

$$\tilde{S}_{SU(3)}(\theta, \sigma_{21}) = \begin{pmatrix} -1 & (\sigma_{12}, 2) & -(\sigma_{12}/2, 1) \\ -(\sigma_{21}, 2) & -1 & -(\sigma_{21}/2, 3) \\ -(\sigma_{21}/2, 3) & -(\sigma_{12}/2, 1) & -1 \end{pmatrix}. \tag{4.12}$$

The S-matrix (4.12) allows for the processes

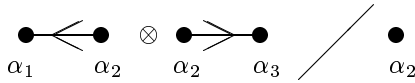
$$2 + 1 \rightarrow (12), \quad 1 + (12) \rightarrow 2, \quad (12) + 2 \rightarrow 1, \tag{4.13}$$

instead of (4.8). Now the fusing angles are read off as

$$\begin{aligned} \eta_{21}^{(12)} &= -i\pi/2 + \sigma_{12}, & \eta_{1(12)}^2 &= -3i\pi/4 - \sigma_{12}/2, \\ \eta_{2(12)}^1 &= -3i\pi/4 - \sigma_{12}/2 \end{aligned} \tag{4.14}$$

and also satisfy (2.10). The masses and decay width are obtained again from (2.1) and (2.2) with $\sigma_{12} \rightarrow \sigma_{21}$. As a whole, we can think of this theory simply as being obtained from the \mathbb{Z}_2 -Dynkin diagram automorphism which exchanges the roles of the particles 1 and 2. However, since parity invariance is now broken this is not a symmetry any more and the two theories are different. In the asymptotic limit $\sigma_{12} \rightarrow \infty$, we obtain once again a simple version of the decoupling rule and the theory decouples into two $SU(2)_2$ models.

We also want to make sense of joining two $SU(3)_2$ theories together when one of the particles is shared, whereas the remaining ones interact trivially. For the choice $\sigma_{21} > 0$ and $\sigma_{23} > 0$ this corresponds algebraically to



Labelling the rows and columns as $\{1, 2, 3, (12), (23)\}$ we can simply associate the following scattering matrix to this model

$$\tilde{S}_{\frac{SU(3) \otimes SU(3)}{SU(2)}} = \begin{pmatrix} -1 & -(\sigma_{12}, 2) & 1 & -(\sigma_{12}/2, 3) & 1 \\ (\sigma_{21}, 2) & -1 & -(\sigma_{32}, 2) & -(\sigma_{21}/2, 1) & -(\sigma_{23}/2, 1) \\ 1 & (\sigma_{23}, 2) & -1 & 1 & -(\sigma_{32}/2, 3) \\ -(\sigma_{21}/2, 1) & -(\sigma_{12}/2, 3) & 1 & -1 & 1 \\ 1 & -(\sigma_{32}/2, 3) & -(\sigma_{23}/2, 1) & 1 & -1 \end{pmatrix}. \tag{4.15}$$

The particle 2 is shared by the two original theories. There is a well-defined limit of this matrix, which is in agreement with the decoupling rule

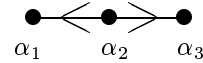
$$\begin{aligned} &\lim_{\sigma_{21} \rightarrow \infty} \tilde{S}_{SU(3) \otimes SU(3)/SU(2)} \\ &= \lim_{\sigma_{23} \rightarrow \infty} \tilde{S}_{SU(3) \otimes SU(3)/SU(2)} = \tilde{S}_{SU(3) \otimes SU(2)}. \end{aligned} \tag{4.16}$$

Similarly, we can construct the remaining three cases of this kind $\sigma_{21} < 0, \sigma_{23} < 0$ or $\sigma_{21} > 0, \sigma_{23} < 0$ or $\sigma_{21} < 0, \sigma_{23} > 0$.

So far we have seen from this example that it is possible to develop a consistent bootstrap and that the outcome depends on the choice of the σ 's. New particles are not predicted from this.

4.1.2 The $SU(4)_2$ -HSG model

In comparison with the previous $SU(3)_2$ model the $SU(4)_2$ model introduces a novel feature. Besides the fundamental unstable particles formed from two stable particles, it also allows for the formation of further unstable particles from the fusing of one unstable particles with a stable one, i.e. secondaries. We start with the case $\sigma_{21} > 0, \sigma_{23} > 0$:



Taking the two parameters of the two $SU(3)_2$ -copies occurring here to $\nu = 1/2$, we proceed analogously as before and have the following bootstrap equations to solve:

$$\begin{aligned} \tilde{S}_{l(12)}(\theta) &= \tilde{S}_{l1} \left(\theta - \frac{\sigma_{21}}{2} + \frac{i\pi}{4} \right) \tilde{S}_{l2} \left(\theta + \frac{\sigma_{21}}{2} - \frac{i\pi}{4} \right), \\ \tilde{S}_{l(23)}(\theta) &= \tilde{S}_{l3} \left(\theta - \frac{\sigma_{23}}{2} + \frac{i\pi}{4} \right) \tilde{S}_{l2} \left(\theta + \frac{\sigma_{23}}{2} - \frac{i\pi}{4} \right), \\ \tilde{S}_{l(123)}(\theta) &= \tilde{S}_{l(12)} \left(\theta + \tilde{\mu}\sigma_{21} - \mu\sigma_{23} + \frac{i\pi}{4} \right) \\ &\quad \times \tilde{S}_{l3} \left(\theta + \frac{2\tilde{\mu} + 1}{2}\sigma_{21} - (1 + \mu)\sigma_{23} - \frac{i\pi}{2} \right), \\ \tilde{S}_{l(123)}(\theta) &= \tilde{S}_{l(23)} \left(\theta + \frac{2\tilde{\mu} + 1}{2}\sigma_{21} - \frac{2\mu + 1}{2}\sigma_{23} + \frac{i\pi}{4} \right) \\ &\quad \times \tilde{S}_{l1} \left(\theta + \frac{2\tilde{\mu} - 1}{2}\sigma_{21} - \mu\sigma_{23} - \frac{i\pi}{2} \right). \end{aligned} \tag{4.17}$$

Here we have already determined several fusing angles by the requirement that the RHS of the last two equations have to be identical. The parameters μ and $\tilde{\mu}$ enter for the same reason as in the previous section and remain in principle free. For simplicity we choose them now as $\mu = -\tilde{\mu} = 1$. As a consistent solution to the bootstrap we then construct

$$\tilde{S}_{SU(4)}(\theta, \sigma_{21}, \sigma_{23}) = \begin{pmatrix} \dots & \cdot & -\left(\frac{\sigma_{23}-2\sigma_{21}}{2}, 3\right) & \left(-\frac{3\sigma_{21}+2\sigma_{23}}{2}, 2\right) \\ \dots & \cdot & \cdot & -1 \\ \dots & -\left(\frac{2\sigma_{32}+\sigma_{21}}{2}, 3\right) & \cdot & \left(-\frac{\sigma_{21}+4\sigma_{23}}{2}, 2\right) \\ \dots & \cdot & 1 & -(\sigma_{21} - \sigma_{23}, 3) \\ * \dots & 1 & \cdot & -\left(-\frac{\sigma_{21}+3\sigma_{23}}{2}, 3\right) \\ * * * & * & * & -1 \end{pmatrix}. \tag{4.18}$$

Here we labeled the rows and columns in the order $\{1, 2, 3, (12), (23), (123)\}$. The particles are all self-conjugate. We abbreviated the entries

$$\bullet \equiv \tilde{S}_{SU(3) \otimes SU(3)/SU(2)}((\sigma_{21} > 0, \sigma_{23} > 0)). \tag{4.19}$$

Note that (4.18) does not completely contain the S-matrix $\tilde{S}_{SU(3)\otimes SU(3)/SU(2)}$, since there are some entries which do not coincide, which indicates that the two $SU(3)$ -copies still interact non-trivially. Only the ones indicated by \bullet are identical to those in (4.15). For conciseness we also did not spell out some entries indicated by “*”. If the * is in the entry \tilde{S}_{ij} , we always report explicitly \tilde{S}_{ji} and the omitted entry can simply be obtained from the crossing relation (2.6). In this case this reads $(\sigma, x) \rightarrow -(-\sigma, 4 - x)$. According to the principles outlined above, the S-matrix (4.18) allows for the processes

$$\begin{aligned} 1 + 2 &\rightarrow (12), & (12) + 1 &\rightarrow 2, \\ 2 + (12) &\rightarrow 1, & 3 + 2 &\rightarrow (23), \\ (23) + 3 &\rightarrow 2, & 2 + (23) &\rightarrow 3, \\ (12) + 3 &\rightarrow (123), & (123) + (12) &\rightarrow 3, \\ 3 + (123) &\rightarrow (12), & (23) + 1 &\rightarrow (123), \\ (123) + (23) &\rightarrow 1, & 1 + (123) &\rightarrow (23). \end{aligned} \tag{4.20}$$

The related fusing angles are read off as

$$\begin{aligned} \eta_{12}^{(12)} &= \sigma_{21} - \frac{i\pi}{2}, & \eta_{(12)1}^2 &= -\frac{\sigma_{21}}{2} - \frac{3i\pi}{4}, \\ \eta_{2(12)}^1 &= -\frac{\sigma_{21}}{2} - \frac{3i\pi}{4}, & \eta_{32}^{(23)} &= \sigma_{23} - \frac{i\pi}{2}, \\ \eta_{(23)3}^2 &= -\frac{\sigma_{23}}{2} - \frac{3i\pi}{4}, & \eta_{2(23)}^3 &= -\frac{\sigma_{23}}{2} - \frac{3i\pi}{4}, \\ \eta_{(12)3}^{(123)} &= \frac{\sigma_{21} - 2\sigma_{23}}{2} - \frac{3i\pi}{4}, \\ \eta_{(123)(12)}^3 &= -\sigma_{21} - \sigma_{23} - \frac{3i\pi}{4}, \\ \eta_{3(123)}^{(12)} &= \frac{\sigma_{21} + 4\sigma_{23}}{2} - \frac{i\pi}{2}, \\ \eta_{(23)1}^{(123)} &= \frac{\sigma_{23} - 2\sigma_{21}}{2} - \frac{3i\pi}{4}, \\ \eta_{(123)(23)}^1 &= \frac{-\sigma_{21} - 3\sigma_{23}}{2} - \frac{3i\pi}{4}, \\ \eta_{1(123)}^{(23)} &= \frac{3\sigma_{21}}{2} + \sigma_{23} - \frac{i\pi}{2}. \end{aligned} \tag{4.21}$$

One verifies that the sum relation of the fusing angles (2.10) holds for all possible processes. The first two lines in (4.20) correspond simply to two copies of $SU(3)_2$ and one does not need to comment further on them. An interesting prediction results from the consideration of the first two processes in the last two lines of (4.20). Making in the first process the particle (12) and in the second the particle (23) stable, by $\sigma_2 \rightarrow \sigma_1$ and by $\sigma_2 \rightarrow \sigma_3$, respectively, both predict the mass of the particle (123) as

$$m_{(123)} \sim me^{|\sigma_{13}|/2}. \tag{4.22}$$

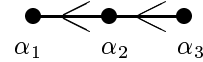
This value is precisely the one we expect from the approximation in the Breit–Wigner formula (2.3). Note that in one case we obtain σ_{13} and in the other σ_{31} as a resonance parameter. The difference results from the fact that according to the processes (4.20), the particle (123) is either

formed as $(1 + 2) + 3$ or $3 + (2 + 1)$. Thus the different parity shows up in this process, but this has no effect on the values for the mass. We also confirm the decoupling rule on the basis of the constructed S-matrix

$$\lim_{\sigma_{21} \rightarrow \infty} \tilde{S}_{SU(4)}(\sigma_{21}, \sigma_{23}) = \tilde{S}_{SU(2)} + \tilde{S}_{SU(3)}(\sigma_{23}), \tag{4.23}$$

$$\lim_{\sigma_{23} \rightarrow \infty} \tilde{S}_{SU(4)}(\sigma_{21}, \sigma_{23}) = \tilde{S}_{SU(3)}(\sigma_{21}) + \tilde{S}_{SU(2)}. \tag{4.24}$$

Similarly we can construct the case $\sigma_{12} > 0, \sigma_{32} > 0$, which leads essentially to a similar qualitative behavior and we can therefore omit its presentation here. More interesting is the case $\sigma_{21} > 0, \sigma_{32} > 0$:



Taking again the two parameters of the $SU(3)_2$ -algebras to $\nu = 1/2$, we proceed analogously as before and have the following bootstrap equations to solve:

$$\begin{aligned} \tilde{S}_{l(12)}(\theta) &= \tilde{S}_{l1} \left(\theta - \frac{\sigma_{21}}{2} + \frac{i\pi}{4} \right) \tilde{S}_{l2} \left(\theta + \frac{\sigma_{21}}{2} - \frac{i\pi}{4} \right), \\ \tilde{S}_{l(23)}(\theta) &= \tilde{S}_{l2} \left(\theta - \frac{\sigma_{32}}{2} + \frac{i\pi}{4} \right) \tilde{S}_{l3} \left(\theta + \frac{\sigma_{32}}{2} - \frac{i\pi}{4} \right), \\ \tilde{S}_{l(123)}(\theta) &= \tilde{S}_{l(12)} \left(\theta - \tilde{\mu}\sigma_{21} - \mu\sigma_{32} + \frac{i\pi}{4} \right) \\ &\quad \times \tilde{S}_{l3} \left(\theta + \frac{1 - 2\tilde{\mu}}{2}\sigma_{21} + (1 - \mu)\sigma_{32} - \frac{i\pi}{2} \right), \\ \tilde{S}_{l(123)}(\theta) &= \tilde{S}_{l1} \left(\theta - \frac{1 + 2\tilde{\mu}}{2}\sigma_{21} - \mu\sigma_{32} - \frac{i\pi}{2} \right) \\ &\quad \times \tilde{S}_{l(23)} \left(\theta + \frac{1 - 2\tilde{\mu}}{2}\sigma_{21} + \frac{1 - 2\mu}{2}\sigma_{32} - \frac{i\pi}{4} \right). \end{aligned} \tag{4.25}$$

Again we have already fixed several fusing angles by the requirement that the RHS of the last two equations have to be identical. The parameters μ and $\tilde{\mu}$ enter for the same reason as in the previous section and remain in principle free. As a consistent solution to the bootstrap we construct now

$$\tilde{S}_{SU(4)}(\theta, \sigma_{21}, \sigma_{32}) = \begin{pmatrix} \bullet \bullet \bullet & \bullet & -\left(-\frac{2\sigma_{21} + \sigma_{32}}{2}, 1\right) & -\left(-\frac{(1 + 2\tilde{\mu})\sigma_{21} + 2\mu\sigma_{32}}{2}, 1\right) \\ \bullet \bullet \bullet & \bullet & \bullet & \frac{1}{\left(\frac{(1 - 2\tilde{\mu})\sigma_{21} + 2(1 - \mu)\sigma_{32}}{2}, 1\right)} \\ \bullet \bullet \bullet & \left(\frac{2\sigma_{32} + \sigma_{21}}{2}, 3\right) & \bullet & \left(\frac{\sigma_{32} + \sigma_{21}}{2}, 2\right)^2 \\ \bullet \bullet \bullet & \bullet & \left(-\tilde{\mu}\sigma_{21} - \mu\sigma_{32}, 3\right) & -\left(\frac{(1 - 2\tilde{\mu})\sigma_{21} + (1 - 2\mu)\sigma_{32}}{2}, 1\right) \\ \bullet \bullet \bullet & \left(-\frac{\sigma_{32} + \sigma_{21}}{2}, 2\right)^2 & \bullet & -\left(\frac{(1 - 2\tilde{\mu})\sigma_{21} + (1 - 2\mu)\sigma_{32}}{2}, 1\right) \\ \bullet \bullet \bullet & \bullet & \bullet & -1 \end{pmatrix}. \tag{4.26}$$

As before, we label the rows and columns in the order $\{1, 2, 3, (12), (23), (123)\}$ and abbreviate the entries

$$\bullet \equiv \tilde{S}_{SU(3)\otimes SU(3)/SU(2)}((\sigma_{21} > 0, \sigma_{32} > 0)). \tag{4.27}$$

The * entries can be obtained in the same way as in (4.18). The S-matrix (4.26) allows for the processes

$$\begin{aligned}
 1 + 2 &\rightarrow (12), & (12) + 1 &\rightarrow 2, \\
 2 + (12) &\rightarrow 1, & 2 + 3 &\rightarrow (23), \\
 3 + (23) &\rightarrow 2, & (23) + 2 &\rightarrow 3, \\
 (12) + 3 &\rightarrow (123), & (123) + (12) &\rightarrow 3, \\
 3 + (123) &\rightarrow (12), & 1 + (23) &\rightarrow (123), \\
 (23) + (123) &\rightarrow 1, & (123) + 1 &\rightarrow (23).
 \end{aligned}
 \tag{4.28}$$

The related fusing angles are read off as

$$\begin{aligned}
 \eta_{12}^{(12)} &= \sigma_{21} - \frac{i\pi}{2}, & \eta_{(12)1}^2 &= -\frac{\sigma_{21}}{2} - \frac{3i\pi}{4}, \\
 \eta_{2(12)}^1 &= -\frac{\sigma_{21}}{2} - \frac{3i\pi}{4}, & \eta_{23}^{(23)} &= \sigma_{32} - \frac{i\pi}{2}, \\
 \eta_{3(23)}^2 &= -\frac{\sigma_{32}}{2} - \frac{3i\pi}{4}, & \eta_{(23)2}^3 &= -\frac{\sigma_{32}}{2} - \frac{3i\pi}{4}, \\
 \eta_{(12)3}^{(123)} &= \frac{2\sigma_{21} + 4\sigma_{32} - 3i\pi}{4}, \\
 \eta_{(123)(12)}^3 &= -\frac{4\tilde{\mu}\sigma_{21} + 4\mu\sigma_{32} + 3i\pi}{4}, \\
 \eta_{3(123)}^{(12)} &= \frac{(2\mu - 2)\sigma_{32} + (2\tilde{\mu} - 1)\sigma_{21} - i\pi}{2}, \\
 \eta_{1(23)}^{(123)} &= \frac{2\sigma_{32} + 4\sigma_{21} - 3i\pi}{4}, \\
 \eta_{(23)(123)}^1 &= \frac{(4\tilde{\mu} - 2)\sigma_{21} + (4\mu - 2)\sigma_{32} - 3i\pi}{4}, \\
 \eta_{(123)1}^{(23)} &= -\frac{(2\tilde{\mu} + 1)\sigma_{21} + \mu\sigma_{32} + i\pi}{2}.
 \end{aligned}
 \tag{4.29}$$

Again one verifies that the relation (2.10) holds for all possible processes. The first two lines in (4.29) correspond again just to two copies of $SU(3)_2$. Also in this case we predict the mass of the particle (123) to correspond to (4.22) making in the first process the particle (12) and in the second the particle (23) stable, by $\sigma_2 \rightarrow \sigma_1$ and by $\sigma_2 \rightarrow \sigma_3$, respectively. There are, however, some fundamental differences with regard to the previous case. First we note that the entries $\tilde{S}_{(12)(23)}(\theta)$ and $\tilde{S}_{(23)(12)}(\theta)$ possess a double pole. We can interpret this as in the case when all particles are stable in terms of the usual Coleman–Thun mechanism [23]. We depict the corresponding fusing structure in Fig. 2. Also the decoupling rule works differently in this case. Now we have $\sigma_{31} > \sigma_{21}, \sigma_{32} > 0$ and due to the non-commutative nature of the limits we obtain a different flow when the resonance parameters are taken to approximate infinity. We note that apart from the \bullet all the entries tend to ± 1 . Thus we also confirm the decoupling rule in the version

$$\lim_{\sigma_{31} \rightarrow \infty} \tilde{S}_{SU(4)}(\sigma_{21}, \sigma_{32}) \sim \tilde{S}_{\frac{SU(3) \otimes SU(3)}{SU(2)}}. \tag{4.30}$$

The case $\sigma_{12} > 0, \sigma_{23} > 0$ is very similar to this one in behavior and does not need to be reported. In summary, we saw in this section that the bootstrap leads to the prediction

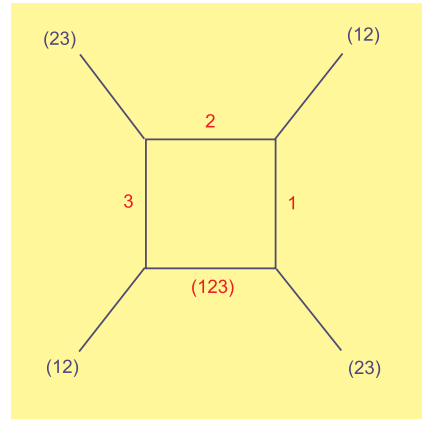


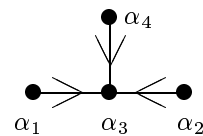
Fig. 2. Coleman–Thun mechanism

of secondary unstable particles with a mass computable from the Breit–Wigner formula. In addition, we saw that by changing the order of the resonance parameters the fusing structure does not merely change with regard to the parity but even develops new pole structures such as double poles.

4.1.3 The $SO(8)_2$ -HSG model

For all models studied so far, we found a one-to-one correspondence between the particle content of the theory and the amount of resonance parameters σ_{ij} with $i < j$ and $i, j \in \{1, \dots, \ell\}$. With regard to the RG scaling functions, which will be computed in the next section, this means that every plateau can be interpreted naturally as related to the onset energy for the excitation of a particle. However, as we already indicated in Sect. 4, this one-to-one correspondence only holds for the $SU(\ell + 1)_2$ -HSG models. For the remaining simply laced algebras it turns out that the dimension of the positive root space is always larger than the amount of parameters σ_{ij} at hand. We study here the simplest example which will exhibit such a behavior, i.e. the $SO(8)_2$ -HSG model. According to (4.5) there are 12 unstable particles, whereas the amount of available resonance parameters is only 10. The following analysis will show that the generalized bootstrap equations we propose provide a satisfactory explanation for this mismatch, in agreement with the previous understanding. We will demonstrate that, in fact, there are 12 particles present in the theory, but the masses of four of them are unavoidably pairwise degenerated. Since both the RG scaling functions and the decoupling rule are determined by the relative mass scales of the particles in the theory, such a degeneracy cannot be unraveled in that context and only 10 particles will be visible.

We consider now the $SO(8)_2$ -HSG model for the choice $\sigma_{13} > 0, \sigma_{23} > 0, \sigma_{43} > 0$ and label the particles as indicated in the Dynkin diagram:



Matching every particle with a positive root of D_4 , we collect the 12 particles in the model in the set

$$\mathcal{P} = \{1, 2, 3, 4, (13), (23), (43), (123), (423), (143), (1234), (12334)\}, \quad (4.31)$$

which allows later for very compact notations. With regard to the previous cases we have a further novelty, namely the occurrence of tertiary unstable particles, i.e. (1234) and (12334). In addition, these two particles exhibit the mentioned mass degeneracy, as we will see later in detail. For the given choice of the resonance parameters we have the bootstrap equations

$$\begin{aligned} \tilde{S}_{l(i3)}(\theta) &= \tilde{S}_{l3} \left(\theta - \frac{\sigma_{i3}}{2} + \frac{i\pi}{4} \right) \tilde{S}_{li} \left(\theta + \frac{\sigma_{i3}}{2} - \frac{i\pi}{4} \right), \\ \tilde{S}_{l(ij3)}(\theta) &= \tilde{S}_{lj} \left(\theta - \frac{\mu_{ij}\sigma_{ji} + 2\sigma_{3j}}{2} + \frac{i\pi}{2} \right) \\ &\quad \times \tilde{S}_{l(i3)} \left(\theta + \frac{\mu_{ij}\sigma_{ij} + \sigma_{i3}}{2} - \frac{i\pi}{4} \right), \\ \tilde{S}_{l(ij3)}(\theta) &= \tilde{S}_{li} \left(\theta - \frac{\mu_{ij}\sigma_{ji} + 2\sigma_{3i}}{2} + \frac{i\pi}{2} \right) \\ &\quad \times \tilde{S}_{l(j3)} \left(\theta + \frac{\mu_{ij}\sigma_{ij} + \sigma_{j3}}{2} - \frac{i\pi}{4} \right), \\ \tilde{S}_{l(1234)}(\theta) &= \tilde{S}_{l(ki3)} \left(\theta - \frac{\mu_{ki}\sigma_{ki} + \mu_{42}\sigma_{24} + \kappa}{2} + \frac{i\pi}{4} \right) \\ &\quad \times \tilde{S}_{lj} \left(\theta + \frac{\mu_{42}\sigma_{42} + \sigma_{j3} - \kappa}{2} - \frac{i\pi}{4} \right), \\ \tilde{S}_{l(12334)}(\theta) &= \tilde{S}_{l(1234)} \left(\theta - \frac{\mu_{42}\sigma_{42} + \sigma_{13} - \kappa + \lambda}{2} + \frac{i\pi}{4} \right) \\ &\quad \times \tilde{S}_{l3} \left(\theta - \frac{\sigma_{13} + \lambda}{2} - \frac{i\pi}{2} \right), \\ \tilde{S}_{l(12334)}(\theta) &= \tilde{S}_{l(j3)} \left(\theta - \frac{\sigma_{1j} + \lambda}{2} + \frac{i\pi}{4} \right) \\ &\quad \times \tilde{S}_{l(ki3)} \left(\theta + \frac{\mu_{ki}\sigma_{ik} + \sigma_{31} - \lambda}{2} - \frac{i\pi}{2} \right). \end{aligned} \quad (4.32)$$

The indices i, j, k can take values in $\{1, 2, 4\}$, such that no two indices are repeated and the associated particles are in \mathcal{P} . This convention will be used throughout this section. The parameters μ_{ij}, κ and λ are in principle free but will be constrained below in order to match consistently the pole structure of \tilde{S} with the corresponding mass spectrum. The entries of the S-matrix can be written in a very compact form, namely

$$\begin{aligned} \tilde{S}_{i(j3)}(\theta) &= (-1)^{\delta_{ij}} \left(\frac{\sigma_{i3} + \sigma_{ij}}{2}, 1 + 2\delta_{i3} \right), \\ \tilde{S}_{i(jk3)}(\theta) &= (-1)^{\delta_{ij} + \delta_{ik}} \left(\frac{\mu_{jk}\sigma_{jk} + 2\sigma_{i3}}{2}, 2 \right), \\ &\quad i \neq 3, \\ \tilde{S}_{(i3)(j3)}(\theta) &= (-1)^{\delta_{ij}}, \end{aligned}$$

$$\begin{aligned} \tilde{S}_{(ij3)(kl3)}(\theta) &= (-1)^{\delta_{ik}\delta_{jl}}, \\ \tilde{S}_{(i3)(jk3)}(\theta) &= -(-1)^{\delta_{ij} + \delta_{ik}} \left(\frac{\mu_{jk}\sigma_{jk} + 2\sigma_{i3}}{2}, 1 \right), \\ \tilde{S}_{(i3)(12334)}(\theta) &= \left(\frac{\sigma_{i1} - \lambda}{2}, 3 \right), \\ \tilde{S}_{(ij3)(1234)}(\theta) &= \left(\frac{\mu_{ij}\sigma_{ji} + \mu_{42}\sigma_{42} - \kappa}{2}, 3 \right), \\ \tilde{S}_{(ij3)(12334)}(\theta) &= - \left(\frac{\mu_{ij}\sigma_{ji} + \sigma_{31} - \lambda}{2}, 3 \right), \\ \tilde{S}_{(1234)(12334)}(\theta) &= \left(\frac{\mu_{42}\sigma_{24} + \sigma_{31} + \kappa - \lambda}{2}, 3 \right), \\ \tilde{S}_{(1234)(1234)}(\theta) &= \tilde{S}_{(12334)(12334)}(\theta) = \tilde{S}_{3(jk3)}(\theta) \\ &= \tilde{S}_{(i3)(1234)}(\theta) = -1. \end{aligned} \quad (4.33)$$

According to the same principles outlined in the previous sections, the physical scattering processes involving the fundamental (primary) unstable particles as well as the corresponding fusing angles are

$$3 + j \rightarrow (j3), \quad (j3) + 3 \rightarrow j, \quad j + (j3) \rightarrow 3, \quad (4.35)$$

$$\begin{aligned} \eta_{3j}^{(j3)} &= \sigma_{j3} - \frac{i\pi}{2}, \quad \eta_{(j3)3}^j = -\frac{\sigma_{j3}}{2} - \frac{3i\pi}{4}, \\ \eta_{j(j3)}^3 &= -\frac{\sigma_{j3}}{2} - \frac{3i\pi}{4}, \end{aligned} \quad (4.36)$$

where we recall that j can take the values 1, 2 and 4, in correspondence with the first equation in (4.32). The processes involving secondary unstable particles are

$$\begin{aligned} j + (k3) &\rightarrow (jk3), \quad (jk3) + j \rightarrow (k3), \\ (k3) + (jk3) &\rightarrow j, \quad k + (j3) \rightarrow (jk3), \\ (jk3) + k &\rightarrow (j3), \quad (j3) + (jk3) \rightarrow k, \end{aligned} \quad (4.37)$$

with $(jk3) \in \mathcal{P}$, such that every secondary unstable particle (123), (423) and (143) can be formed in two different processes. The associated fusing angles can also be written in a closed form

$$\begin{aligned} \eta_{j(k3)}^{(jk3)} &= \frac{2(\sigma_{3j} + \sigma_{jk}) - 3i\pi}{4}, \\ \eta_{(jk3)j}^{(k3)} &= \frac{\mu_{jk}\sigma_{jk} + 2\sigma_{k3} - i\pi}{2}, \\ \eta_{(k3)(jk3)}^j &= \frac{2(\mu_{jk}\sigma_{kj} + 2\sigma_{3k}) - 3i\pi}{4}, \\ \eta_{k(j3)}^{(jk3)} &= \frac{2(\sigma_{3k} + \sigma_{kj}) - 3i\pi}{4}, \\ \eta_{(jk3)k}^{(j3)} &= \frac{\mu_{jk}\sigma_{jk} + 2\sigma_{j3} - i\pi}{2}, \\ \eta_{(j3)(jk3)}^k &= \frac{2(\mu_{jk}\sigma_{kj} + 2\sigma_{3j}) - 3i\pi}{4}. \end{aligned} \quad (4.38)$$

Finally, the processes which involve the tertiary unstable particles (1234) and (12334) are

$$\begin{aligned}
 (kl3) + j &\rightarrow (1234), \quad (1234) + (kl3) \rightarrow j, \\
 j + (1234) &\rightarrow (kl3), \quad (j3) + (kl3) \rightarrow (12334), \\
 (kl3) + (12334) &\rightarrow (j3), \quad (12334) + (j3) \rightarrow (kl3), \\
 (1234) + 3 &\rightarrow (12334), \\
 3 + (12334) &\rightarrow (1234), \\
 (12334) + (1234) &\rightarrow 3,
 \end{aligned} \tag{4.39}$$

with fusing angles

$$\begin{aligned}
 \eta_{(kl3)j}^{(1234)} &= \frac{\mu_{kl}\sigma_{kl} + 2\sigma_{j3} - i\pi}{2}, \\
 \eta_{(1234)(kl3)}^j &= \frac{2(\mu_{kl}\sigma_{lk} + \mu_{42}\sigma_{42} - \kappa) - 3i\pi}{4}, \\
 \eta_{j(1234)}^{(kl3)} &= \frac{2(\mu_{42}\sigma_{24} + \kappa + 2\sigma_{3j}) - 3i\pi}{4}, \\
 \eta_{(j3)(kl3)}^{(12334)} &= \frac{2(\mu_{kl}\sigma_{lk} + 2\sigma_{3j}) - 3i\pi}{4}, \\
 \eta_{(kl3)(12334)}^{(j3)} &= \frac{\mu_{kl}\sigma_{kl} + \sigma_{13} + \lambda - i\pi}{2}, \\
 \eta_{(12334)(j3)}^{(kl3)} &= \frac{2(\sigma_{j1} - \lambda) - 3i\pi}{4}, \\
 \eta_{(1234)3}^{(12334)} &= \frac{2(\mu_{42}\sigma_{42} - \kappa) - 3i\pi}{4}, \\
 \eta_{3(12334)}^{(1234)} &= \frac{\sigma_{13} + \lambda - i\pi}{2}, \\
 \eta_{(12334)(1234)}^3 &= \frac{2(\mu_{42}\sigma_{24} + 2\sigma_{31} - \lambda + \kappa) - 3i\pi}{4}.
 \end{aligned}$$

Similarly as for the $SU(4)_2$ -HSG model studied before, one of the main predictions, which supports the working of our proposal, are the masses of the unstable particles. In the case of the present theory, this predictive power is especially important, since we intend to show the degeneracy of some of these masses. For the secondary unstable particles we can proceed as in the previous sections and consider the processes $j + (k3)$ and $k + (j3)$ for fixed j, k and make the primary unstable particles stable. By looking at the corresponding fusing angles we find

$$\left. \begin{aligned}
 \lim_{\sigma_3 \rightarrow \sigma_k} j + (k3) &\rightarrow (jk3) \\
 \lim_{\sigma_3 \rightarrow \sigma_j} k + (j3) &\rightarrow (jk3)
 \end{aligned} \right\} \Rightarrow m_{(jk3)} \sim me^{|\sigma_{jk}|/2}, \tag{4.40}$$

that is, the masses of the secondary unstables are predicted once more according to (2.3). Most interesting is the analysis for the next generation of unstable particles, the tertiaries.

Let us consider the formation process for the particle (1234). We have to look at the processes $(jk3) + l \rightarrow (1234)$

with $j, k, l \equiv \{1, 2, 4\}$ such that $(jk3) \in \mathcal{P}$,

$$\left. \begin{aligned}
 \lim_{\sigma_3 \rightarrow \sigma_k} j + (k3) &\rightarrow (jk3) + l \\
 \lim_{\sigma_3 \rightarrow \sigma_j} k + (j3) &\rightarrow (jk3) + l
 \end{aligned} \right\} \rightarrow (1234) \Rightarrow m_{(1234)} \sim \sqrt{2}me^{\frac{|\sigma_{13}|}{2}}. \tag{4.41}$$

This equation requires some comments. Reading (4.41) for each individual value of l , we end up with the condition $\sigma_k = \sigma_j = \sigma_3$ for $j, k \in \{1, 2, 4\} \neq l$. This should hold for all values of l , such that when we demand the uniqueness of the mass $m_{(1234)}$ we end up with the condition $\sigma_1 = \sigma_2 = \sigma_3 = \sigma_4$. This means

$$m_{(1234)} \sim \sqrt{2}m, \tag{4.42}$$

and the particle (1234) will also be invisible in any RG flow. Let us now consider the tertiary particle (12334). The processes to be investigated are the ones listed above in (4.39)

$$\left. \begin{aligned}
 \lim_{\sigma_3 \rightarrow \sigma_k} j + (k3) &\rightarrow (jk3) + l \\
 \lim_{\sigma_3 \rightarrow \sigma_j} k + (j3) &\rightarrow (jk3) + l
 \end{aligned} \right\} \rightarrow \sigma_l \rightarrow \sigma_3(1234) + 3 \rightarrow (12334) \Rightarrow m_{(12334)} \sim m, \tag{4.43}$$

$$\left. \begin{aligned}
 \lim_{\sigma_l \rightarrow \sigma_3} (l3) + \lim_{\sigma_3 \rightarrow \sigma_k} j + (k3) \\
 \lim_{\sigma_3 \rightarrow \sigma_j} k + (j3)
 \end{aligned} \right\} \rightarrow (l3) + \sigma_j \rightarrow \sigma_k(jk3) \rightarrow (12334) \Rightarrow m_{(12334)} \sim m. \tag{4.44}$$

We presented here the complete chain of processes leading to the formation of the unstable particle (12334). As can be seen from (4.44) and (4.43), making all intermediate particles stable amounts to the equality of all resonance parameters, so that there is no σ -dependence in the final expression for the mass. Therefore, with regard to the mass spectrum, the particle (12334) is indistinguishable from the stable particles in the theory.

Due to the fact that the formation of (1234) and (12334) requires all resonance parameters to be equal, the parameters κ and λ can never be fixed by the mass analysis. Similarly the parameters μ_{ij} can also not be constrained further by means of the mass analysis. However, there is still a further check to be carried out, namely the decoupling rule. For the choice mentioned $\sigma_{13} > 0, \sigma_{23} > 0, \sigma_{43} > 0$ we expect to find the following decoupling flow:

$$\begin{aligned}
 &\lim_{\sigma_{43}, \sigma_{23}, \sigma_{13} \rightarrow \infty} \tilde{S}_{SO(8)}(\sigma_{13}, \sigma_{23}, \sigma_{43}) \\
 &= \lim_{\sigma_{43}, \sigma_{23} \rightarrow \infty} \tilde{S}_{SU(4)}(\sigma_{23}, \sigma_{43}) + \tilde{S}_{SU(2)} \\
 &= \lim_{\sigma_{43} \rightarrow \infty} \tilde{S}_{SU(3)}(\sigma_{43}) + \tilde{S}_{SU(2)} + \tilde{S}_{SU(2)} \\
 &= \tilde{S}_{SU(2)} + \tilde{S}_{SU(2)} + \tilde{S}_{SU(2)}.
 \end{aligned} \tag{4.45}$$

In order to achieve consistency of \tilde{S} with (4.45) the following constraints have to be satisfied:

$$\begin{aligned}
|\mu_{ij}| &> 2, \\
|\kappa_1| &> 2, \quad |\kappa_2| > 0, \quad |\kappa_4| > 0, \\
|\lambda_2| &> 1, \quad |\lambda_4| > 1, \quad |\lambda_1| > 0, \\
|\kappa_1 + \mu_{12}| &> 0, \quad |\kappa_1 + \mu_{14}| > 0, \\
|\kappa_2 + \mu_{42}| &> 2, \quad |\kappa_2 - \mu_{12}| > 0, \\
|\kappa_4 + \mu_{42}| &> 0, \quad |\kappa_4 - \mu_{42}| > 2, \\
|\lambda_1 - \kappa_1 + 1| &> 0, \quad |\lambda_1 + \mu_{14} + 1| > 0, \\
|\lambda_1 + \mu_{12} + 1| &> 0, \\
|\lambda_2 - \kappa_2 - \mu_{42}| &> 0, \quad |\lambda_2 - \mu_{12}| > 0, \\
|\lambda_2 - \mu_{42}| &> 0, \\
|\lambda_4 - \kappa_4 + \mu_{42}| &> 0, \quad |\lambda_4 - \mu_{42}| > 0, \\
|\lambda_4 - \mu_{14}| &> 0,
\end{aligned} \tag{4.46}$$

for

$$\begin{aligned}
\kappa &= \kappa_1\sigma_{13} + \kappa_2\sigma_{23} + \kappa_4\sigma_{43} \quad \text{and} \\
\lambda &= \lambda_1\sigma_{13} + \lambda_2\sigma_{23} + \lambda_4\sigma_{43}.
\end{aligned} \tag{4.47}$$

A possible, but not unique, choice which allows one to satisfy the conditions (4.46) is

$$\mu_{ij} = \kappa_1 = \lambda_1 = 5/2, \quad \lambda_2 = \lambda_4 = 3/2$$

and

$$\kappa_4 = \kappa_2 = 7/2. \tag{4.48}$$

We summarize the main new observations from this example: Tertiary unstable particles can be formed, but in this case they are unavoidably mass degenerate in comparison with a primary and a stable particle.

4.2 Thermodynamic Bethe ansatz analysis

In this section we want to compare the findings of the previous section with an alternative method. We employ for this the thermodynamic Bethe ansatz [24] in order to compute the scaling function in dependence of the inverse temperature. One should stress that the only input into this approach is the proper S-matrix involving stable particles and not \tilde{S} . As discussed in [11] for the first time for the HSG models, we expect to find the typical staircase pattern, in which each step can be related to the energy scale of the formation of at least an unstable particle. The central equations to solve in this context are the TBA equations

$$rm_a^i \cosh \theta = \varepsilon_a^i(\theta) + \sum_{b=1}^{\ell} \sum_{j=1}^{\tilde{\ell}} \Phi_{ab}^{ij} * L_b^j(\theta). \tag{4.49}$$

By the symbol “*” we denote the rapidity convolution of two functions defined as $f * g(\theta) := \int d\theta' / 2\pi f(\theta - \theta')g(\theta')$.

The renormalization group parameter r is related to the temperature T by $r = m/T$, where m is the mass scale of the lightest particle. We also re-defined the masses as usual by $m_a^i \rightarrow m_a^i/m$. The pseudo-energies $\varepsilon_a^i(\theta)$ are related to the functions $L_b^j(\theta) = \ln(1 + e^{-\varepsilon_b^j(\theta)})$. The kernels in the integrals carry the information of the dynamical interaction of the system and are given by

$$\Phi_{ab}^{ij}(\theta) = -i \frac{d}{d\theta} \ln S_{ab}^{ij}(\theta). \tag{4.50}$$

Recall that in general we characterize the particles by two quantum numbers (a, i) as explained in Sect. 3, unlike in the last sections where we could drop one as we were dealing with level 2 only. For instance for the $\tilde{\mathfrak{g}}_2$ -HSG scattering matrix (4.3) the kernel simply reads

$$\Phi^{ij}(\theta) = \tilde{I}_{ij} \cosh^{-1}(\theta + \sigma_{ij}), \tag{4.51}$$

with \tilde{I} being the incidence matrix of $\tilde{\mathfrak{g}}$. Having solved the equations (4.49) for the pseudo-energies $\varepsilon_i(\theta)$ one can compute the scaling function

$$c(r) = \frac{3r}{\pi^2} \sum_{i,a} m_a^i \int_0^{\infty} d\theta \cosh \theta (L_a^i(\theta) + L_a^i(-\theta)). \tag{4.52}$$

Due to its non-linear nature the TBA equations are known not to be solvable analytically, albeit in certain regions analytical approximations exist. We shall now solve these equations numerically. According to the above discussion we are particularly interested in higher rank Lie algebras, since the decoupling rule (3.4) will be most complex in that case. Even though solving (4.49) numerically is a relatively simple iteration problem, its full solution for high ranks requires a considerable computational effort. In order to tackle such situations a sophisticated procedure has been developed [25], which allows one to compute in a reasonable short time high rank scaling functions to a very high precision.

However, in many cases one can use some standard techniques, see e.g. [11, 24], and approximate (4.49) by the so-called constant TBA equations and predict the values for c . In a large regime for θ , when r is small, one may approximate $\varepsilon_a^i(\theta) = \varepsilon_a^i = \text{const}$. By standard TBA arguments [24] it follows that the effective central charge is expressible as

$$c_{\text{eff}} = \frac{6}{\pi^2} \sum_{a=1}^{\ell} \sum_{i=1}^{\tilde{\ell}} \mathcal{L} \left(\frac{x_a^i}{1 + x_a^i} \right), \quad x_a^i = \prod_{b=1}^{\ell} \prod_{j=1}^{\tilde{\ell}} (1 + x_b^j)^{N_{ab}^{ij}}, \tag{4.53}$$

with $\mathcal{L}(x) = \sum_{n=1}^{\infty} x^n / n^2 + \ln x \ln(1-x)/2$ denoting Rogers dilogarithm,

$$x_a^i = \exp(-\varepsilon_a^i) \quad \text{and} \quad N_{ab}^{ij} = 1/2\pi \int_{-\infty}^{\infty} d\theta \Phi_{ab}^{ij}(\theta).$$

We will exploit this fact below.

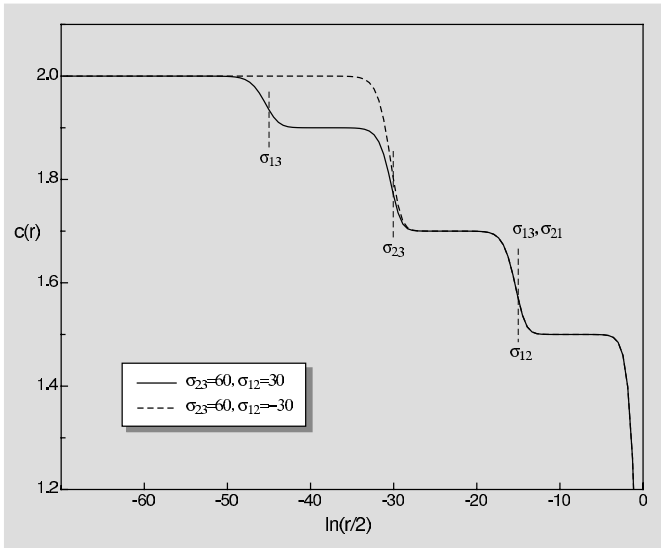


Fig. 3. The $SU(4)_2$ RG flow

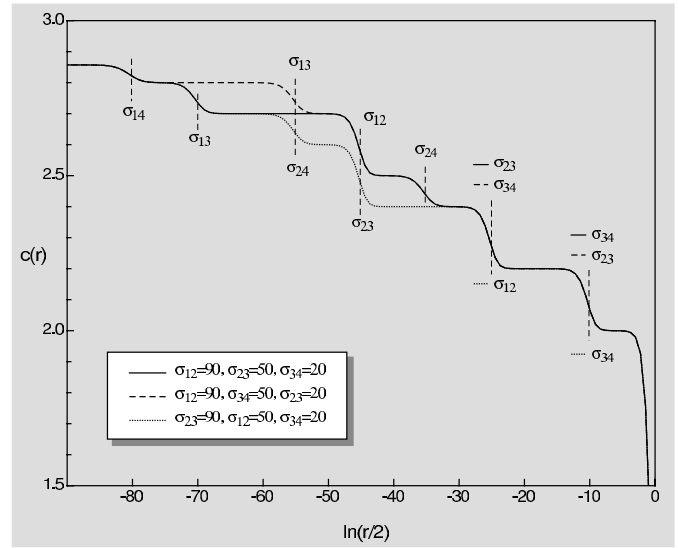


Fig. 4. The $SU(5)_2$ RG flow

4.2.1 The $SU(4)_2$ -HSG model

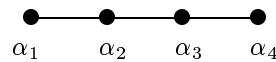
As already discussed as an example in Sects. 3.1 and 3.2.2, we have two qualitatively different behaviors for this case. For the ordering $\sigma_{21} > 0, \sigma_{23} > 0$ we expect to find three plateaus in the scaling function, whereas the ordering $\sigma_{21} > 0, \sigma_{32} > 0$ is associated to a different decoupling rule with four plateaus. This is the behavior the decoupling rule predicts and which we already saw confirmed when taking the limits of the scattering matrix obtained from our bootstrap proposal. In addition we now also find this behavior being validated with a TBA analysis. Figure 3 contains the numerical outcome of the solutions of (4.49) and (4.52) and agrees with our expectations. Note that we do not only predict correctly the height of the plateaus, but also their onset at $\ln(r/2) \sim \sigma/2$, which is in agreement with the approximation to the Breit–Wigner formula (2.3). From this analysis we can now support our reasoning with regard to the comment on the occurrence of the absolute value in the Breit–Wigner formula. The two cases presented in Fig. 3 only differ by the signs of the resonance parameter σ_{12} and are evidently not identical. In one case we have $\sigma_{13} = \sigma_{12} + \sigma_{23} = 90$ leading to an additional plateau and in the other we have $\sigma_{13} = \sigma_{12} + \sigma_{23} = 30$, which does not give an onset related to σ_{13} as the decoupling between the vertices 1 and 2 already took place.

These findings seem to contradict some result previously obtained from a form factor analysis [20]. In there as in all previous publications on the subject, e.g. [10, 11], an absolute value was used in the Breit–Wigner formula, such that the signs of the resonance parameters were handled quite casual. In fact, the results presented in Fig. 1 in [20] for $SU(4)_2$ correspond to the values $\sigma_{12} = 50, \sigma_{23} = -20$ rather than $\sigma_{12} = 50, \sigma_{23} = 20$ which agrees with the decoupling rule. Likewise matters are clarified below for the $SU(5)_2$ -HSG case.

The occurrence of additional plateaus which could not be associated to primary unstable particles for several algebras was noted in [25]. Their occurrence in the $SU(4)_2, SU(5)_2, SO(8)_2$ -HSG models, as will also be discussed in the next section, was also commented upon in [26]. This latter observation was only based on a TBA-calculation of the finite size scaling function. In [26] the statement was made that these further plateaus could possibly be related to “new” unstable particles in the spectrum. However, predictive rules for the fixed points of the RG flow such as the decoupling rule (3.4) and also for the on-set as the bootstrap principle, which we both provide here, were absent.

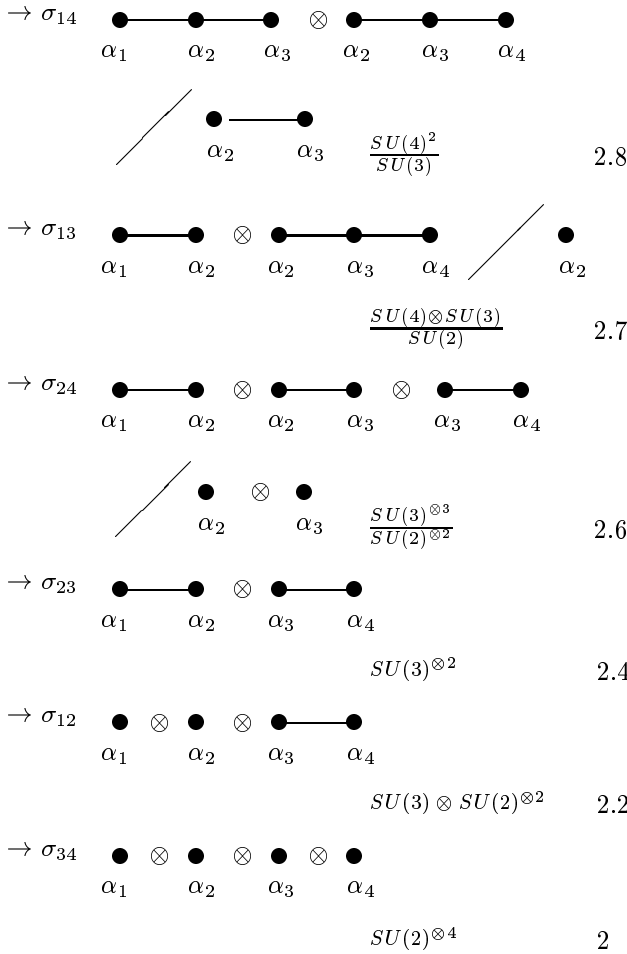
4.2.2 The $SU(5)_2$ -HSG model

This case already allows for many more possibilities, that is, potentially $6!$ different orderings of the resonance parameters. Let us discuss one case in more detail and present two more in a shorter form. We choose the values for the resonance parameters directly associated to the links of the Dynkin diagram, i.e. the primary unstables, as $\sigma_{23} = 90, \sigma_{12} = 50, \sigma_{34} = 20$, such that the remaining parameters result in $\sigma_{14} = 160, \sigma_{13} = 140, \sigma_{24} = 110$. According to the decoupling rule we can then predict the renormalization group flow. We report here the flow from the ultraviolet to the infrared, indicating the resonance parameters responsible for the particular onsets together with the Dynkin diagrams of the new underlying algebra and their related Lie groups and Virasoro central charges:



$SU(5)$

$\frac{20}{7} \sim 2.86$



Comparing this computation with the numerical outcome of our TBA analysis, depicted in Fig. 4, reproduces very well this flow in form of the dotted line together with the onset at $\ln(r/2) \sim \sigma/2$ for each resonance parameter. Note the explicit occurrence of the secondary unstable particles. The other two examples presented in Fig. 4 are

$$\begin{aligned}
 & SU(5) && 20/7 \sim 2.86 \\
 \rightarrow \sigma_{14} = 160/\sigma_{14} = 160 & & & \\
 & SU(4)^{\otimes 2}/SU(3) && 2.8 \\
 \rightarrow \sigma_{13} = 140/\sigma_{13} = 110 & & & \\
 & SU(4) \otimes SU(3)/SU(2) && 2.7 \\
 \rightarrow \sigma_{12} = 90/\sigma_{12} = 90 & & & \\
 & SU(4) \otimes SU(2) && 2.5 \\
 \rightarrow \sigma_{24} = 70/\sigma_{24} = 70 & & & \\
 & SU(3)^{\otimes 2} \otimes SU(2)/SU(2) && 2.4 \\
 \rightarrow \sigma_{23} = 50/\sigma_{34} = 50 & & & \\
 & SU(3) \otimes SU(2)^{\otimes 2} && 2.2 \\
 \rightarrow \sigma_{34} = 20/\sigma_{23} = 20 & & & \\
 & SU(2)^{\otimes 4} && 2
 \end{aligned}
 \tag{4.54}$$

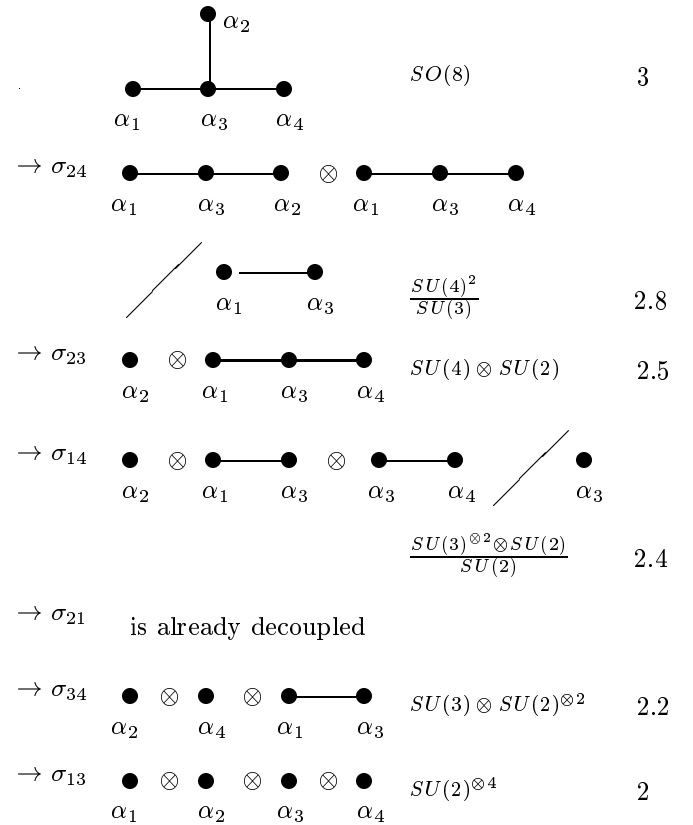
Note that both orderings in (4.54) give rise to the same flows which is once again in agreement with the decoupling rule. The difference between these two orderings is, however, that we are dealing with theories which contain different mass spectra of the unstable particles, such that the onset varies in both cases according to (2.3).

4.2.3 The $SO(8)_2$ -HSG model

Being a rank 4 algebra as the previous example, also in this case we have potentially 6! different orderings of the resonance parameters. Let us study this case for the ordering

$$\begin{aligned}
 \sigma_{24} = 140 > \sigma_{23} = 90 > \sigma_{21} = \sigma_{14} = 70 > \sigma_{34} = 50 \\
 > \sigma_{13} = 20.
 \end{aligned}
 \tag{4.55}$$

Then, according to the decoupling rule, we predict the flow



From the decoupling at σ_{14} we observe that it is important to keep track of the simple root labels on the vertices. The cancellation will be different depending on if one decouples next with σ_{13} or σ_{34} . The presented values for the RG fixed points may be compared with the dotted line in Fig. 5, which is again the numerical outcome of a TBA analysis. We present two more flows in Fig. 5. Once again the two different orderings lead to the same flows, but the onsets vary according to (2.3). An important fact to notice from all graphs is that we only observe the primary and secondary unstables in this analysis and the tertiaries remain invisible.

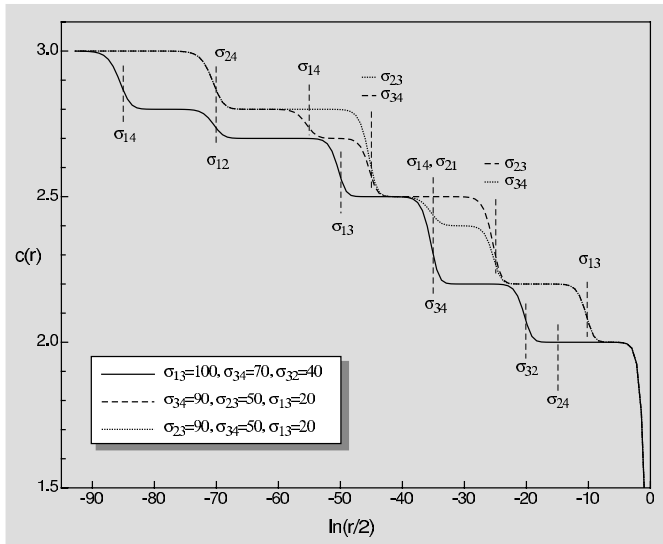


Fig. 5. The $SO(8)_2$ RG flow

This is in agreement with our bootstrap analysis in Sect. 3.2.3, which provides a consistent explanation of the claim that all positive roots but the simple ones should be related to unstable particles:

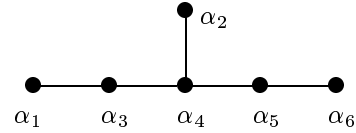
$SO(8)$	3
$\rightarrow \sigma_{14} = 170/\sigma_{24} = 140$	
$SU(4)^{\otimes 2}/SU(3)$	2.8
$\rightarrow \sigma_{12} = 140/\sigma_{14} = 110$	
$SU(4) \otimes SU(3)/SU(2)$	2.7
$\rightarrow \sigma_{13} = 100/\sigma_{34} = 90$	(4.56)
$SU(4) \otimes SU(2)$	2.5
$\rightarrow \sigma_{34} = 70/\sigma_{23} = 50$	
$SU(2)^{\otimes 2} \otimes SU(3)$	2.2
$\rightarrow \sigma_{21} = 30$	is already decoupled
$\rightarrow \sigma_{32} = 40/\sigma_{13} = 20$	
$SU(2)^{\otimes 4}$	2
$\rightarrow \sigma_{24} = 30$	is already decoupled

In summary, we conclude from this section that the number of unstable particles is actually 12, in agreement with (4.5), but for the mentioned reason only 10 can be seen in the RG flow.

4.2.4 The $(E_6)_2$ -HSG model

In this case we have already 15! different possible orderings. We want to present two more explicit examples, which will be instructive since in comparison with the previous ones they add more non-trivial structure, namely mass degeneracy. Note that this degeneracy is not the unavoidable one of

the tertiary unstables as discussed in the previous section, but it arises through the particular choice of the primary resonance parameters. This is nonetheless instructive as we will demonstrate that the decoupling rule also works well in that case. We label the particles as indicated in the following Dynkin diagram:



We choose once again first the ordering for the primary resonance parameters

$$\sigma_{13} = 100 > \sigma_{34} = 80 > \sigma_{45} = 60 > \sigma_{56} = 40 > \sigma_{24} = 20. \tag{4.57}$$

According to the decoupling rule we predict then the flow:

E_6	$\frac{36}{7} \sim 5.14$
$\rightarrow \sigma_{16} = 280$	
$SO(10)^{\otimes 2}/SO(8)$	5
$\rightarrow \sigma_{15} = 240$	
$SO(10) \otimes SU(5)/SU(4)$	$\frac{34}{7} \sim 4.86$
$\rightarrow \sigma_{14} = \sigma_{36} = 180$	
$SO(8) \otimes SU(5) \otimes SU(3)/SU(4) \otimes SU(2)$	$\frac{319}{70} \sim 4.56$
$\rightarrow \sigma_{12} = 160$	is already decoupled
$\rightarrow \sigma_{35} = 140$	
$SU(5) \otimes SU(4) \otimes SU(3)/SU(3) \otimes SU(2)$	$\frac{61}{14} \sim 4.36$
$\rightarrow \sigma_{26} = 120$	(4.58)
$SU(4)^{\otimes 3} \otimes SU(3)/SU(3)^{\otimes 2} \otimes SU(2)$	4.3
$\rightarrow \sigma_{13} = \sigma_{46} = 100$	
$SU(4)^{\otimes 2} \otimes SU(3) \otimes SU(2)/SU(3) \otimes SU(2)4$	
$\rightarrow \sigma_{25} = \sigma_{34} = 80$	
$SU(3)^{\otimes 3} \otimes SU(2)^{\otimes 2}/SU(2)^{\otimes 2}$	3.6
$\rightarrow \sigma_{32} = \sigma_{45} = 60$	
$SU(3)^{\otimes 2} \otimes SU(2)^{\otimes 2}$	3.4
$\rightarrow \sigma_{56} = 40$	
$SU(3) \otimes SU(2)^{\otimes 4}$	3.2
$\rightarrow \sigma_{24} = 20$	
$SU(2)^{\otimes 6}$	3

These analytical predictions are well confirmed with the outcome of our TBA analysis as presented by the solid line in Fig. 6. Note that eight particles are pairwise degenerate

$$S = \begin{pmatrix} [2]_0^{-1} & e^{-\frac{i\pi}{3}}[1]_{\sigma_{12}} & 1 & -[1]_0^{-1} & e^{-\frac{2\pi i}{3}}[2]_{\sigma_{12}} & 1 \\ e^{\frac{i\pi}{3}}[1]_{\sigma_{21}} & [2]_0^{-1} & e^{-\frac{i\pi}{3}}[1]_{\sigma_{23}} & e^{\frac{2\pi i}{3}}[2]_{\sigma_{21}} & -[1]_0^{-1} & e^{-\frac{2\pi i}{3}}[2]_{\sigma_{23}} \\ 1 & e^{\frac{i\pi}{3}}[1]_{\sigma_{32}} & [2]_0^{-1} & 1 & e^{\frac{2\pi i}{3}}[2]_{\sigma_{32}} & -[1]_0^{-1} \\ -[1]_0^{-1} & e^{-\frac{2\pi i}{3}}[2]_{\sigma_{12}} & 1 & [2]_0^{-2}[4]_0^{-1} & -e^{-\frac{i\pi}{3}}[1]_{\sigma_{12}} & 1 \\ e^{\frac{2\pi i}{3}}[2]_{\sigma_{21}} & -[1]_0^{-1} & e^{-\frac{2\pi i}{3}}[2]_{\sigma_{23}} & -e^{\frac{i\pi}{3}}[1]_{\sigma_{21}} & [2]_0^{-2}[4]_0^{-1} & -e^{-\frac{i\pi}{3}}[1]_{\sigma_{23}} \\ 1 & e^{\frac{2\pi i}{3}}[2]_{\sigma_{32}} & -[1]_0^{-1} & 1 & -e^{\frac{i\pi}{3}}[1]_{\sigma_{32}} & [2]_0^{-2}[4]_0^{-1} \end{pmatrix} \quad (4.61)$$

and we therefore expect to find $15 - 8/2 = 11$ plateaus in the flow. The first step which corresponds to one of these degeneracies occurs for instance at $\sigma_{14} = \sigma_{36}$ and we have to apply the decoupling rule twice at this point. The dashed line corresponds to the flow

E_6	$\frac{36}{7} \sim 5.14$
$\rightarrow \sigma_{16} = 280$	
$SO(10)^{\otimes 2}/SO(8)$	5
$\rightarrow \sigma_{15} = 240$	
$SO(10) \otimes SU(5)/SU(4)$	$\frac{34}{7} \sim 4.86$
$\rightarrow \sigma_{36} = 220$	
$SU(5)^{\otimes 2} \otimes SO(8)/SU(4)^{\otimes 2}$	$\frac{33}{7} \sim 4.71$
$\rightarrow \sigma_{35} = 180$	
$SU(5)^{\otimes 2}/SU(3)$	$\frac{158}{35} \sim 4.51$
$\rightarrow \sigma_{26} = 160$	
$SU(4)^{\otimes 2} \otimes SU(5)/SU(3)^{\otimes 2}$	$\frac{156}{35} \sim 4.46$
$\rightarrow \sigma_{14} = \sigma_{46} = 140$	(4.59)
$SU(4)^{\otimes 2} \otimes SU(3)^{\otimes 2}/SU(2)^{\otimes 2} \otimes SU(3)$	4.2
$\rightarrow \sigma_{12} = \sigma_{25} = 120$	
$SU(4) \otimes SU(3)^{\otimes 3}/SU(2)^{\otimes 3}$	4.1
$\rightarrow \sigma_{45} = 100$	
$SU(4) \otimes SU(3)^{\otimes 2}/SU(2)$	3.9
$\rightarrow \sigma_{34} = 80$	
$SU(3)^{\otimes 3}$	3.6
$\rightarrow \sigma_{13} = \sigma_{32} = 60$	
$SU(3)^{\otimes 2} \otimes SU(2)^{\otimes 2}$	3.4
$\rightarrow \sigma_{56} = 40$	
$SU(3) \otimes SU(2)^{\otimes 4}$	3.2
$\rightarrow \sigma_{24} = 20$	
$SU(2)^{\otimes 6}$	3

Now only six particles are pairwise degenerate and we expect to find $15 - 6/2 = 12$ plateaus, which is precisely what

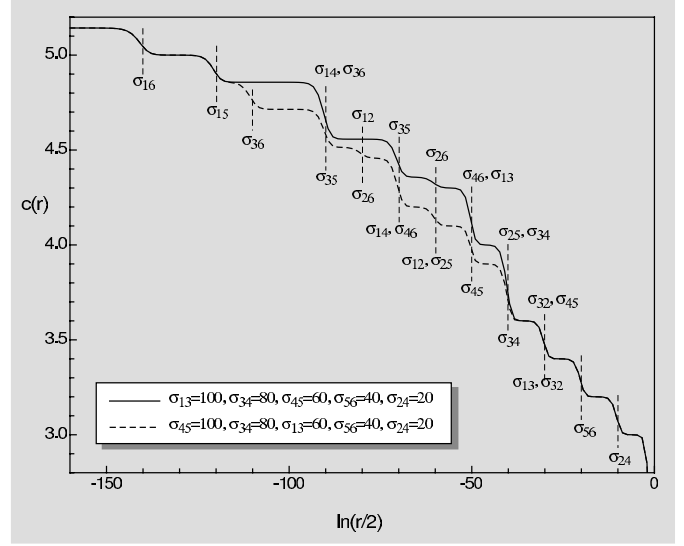


Fig. 6. The $(E_6)_2$ RG flow

we see in Fig. 6. Overall we have seen in this section that even for this involved case the decoupling rule is confirmed.

4.2.5 The $SU(4)_3$ -HSG model

In order to support the working of the decoupling rule also for higher level algebras we will now consider one level 3 example, i.e. $SU(4)_3$. In this model we have six particles. When labeling the rows and columns in the order $\{(1, 1), (1, 2), (1, 3), (2, 1), (2, 2), (2, 3)\}$, the scattering matrix in this case reads (see above, (4.61)) where we abbreviated $[x]_\sigma := \sinh \frac{1}{2} (\theta + \sigma - \frac{i\pi x}{3}) / \sinh \frac{1}{2} (\theta + \sigma + \frac{i\pi x}{3})$. As in the previous cases we can now solve the TBA equations numerically and according to the fusing rule we expect as in the level 2 case either 3 or 4 plateaus depending on the ordering $\sigma_{21} > 0, \sigma_{23} > 0$ or $\sigma_{21} > 0, \sigma_{32} > 0$, respectively.

$SU(4)_3$	$\frac{24}{7} \sim 3.49$
$\rightarrow \sigma_{23} = 60$	
$SU(2)_3 \otimes SU(3)_3$	2.8
$\rightarrow \sigma_{21} = 30$	
$(SU(2)_3)^{\otimes 3}$	2.4
or	
$SU(4)_3$	$\frac{24}{7} \sim 3.49$ (4.61)

$$\begin{aligned}
 &\rightarrow \sigma_{13} = 90 \\
 (SU(3)_3)^{\otimes 2} / SU(2)_3 & \quad 3.2 \\
 &\rightarrow \sigma_{23} = 60 \\
 SU(2)_3 \otimes SU(3)_3 & \quad 2.8 \\
 &\rightarrow \sigma_{12} = 30 \\
 (SU(2)_3)^{\otimes 3} & \quad 2.4
 \end{aligned}$$

Indeed Fig. 7 confirms this behavior in the form of the solid and dashed line. Unfortunately, the iterative procedure used for solving the TBA equations ceases to converge when we reach the value $\ln(r/2)$ equal to the highest resonance parameter in both cases. Nonetheless, the highest plateau may be computed analytically simply from the constant TBA equations (4.53). In Fig. 7 we indicate these analytical values, which we cannot obtain numerically at present, by the dotted lines. The other RG fixed points may be computed similarly. We evaluate

$$\begin{aligned}
 x_1^1 = x_2^1 = x_1^3 = x_2^3 &= \frac{\sin\left(\frac{2\pi}{7}\right) \sin\left(\frac{4\pi}{7}\right)}{\sin\left(\frac{\pi}{7}\right) \sin\left(\frac{5\pi}{7}\right)} - 1, \\
 x_1^2 = x_2^2 &= \frac{\sin^2\left(\frac{3\pi}{7}\right)}{\sin\left(\frac{\pi}{7}\right) \sin\left(\frac{5\pi}{7}\right)} - 1,
 \end{aligned} \tag{4.62}$$

$$\begin{aligned}
 c_{\text{eff}} &= \frac{6}{\pi^2} \left[4\mathcal{L}\left(\frac{x_1^1}{1+x_1^1}\right) + 2\mathcal{L}\left(\frac{x_2^2}{1+x_2^2}\right) \right] \\
 &= \frac{24}{7} \sim 3.43.
 \end{aligned} \tag{4.63}$$

The important fact here is the confirmation of the decoupling rule for higher levels, sustained by the occurrence of the additional plateau at 3.2.

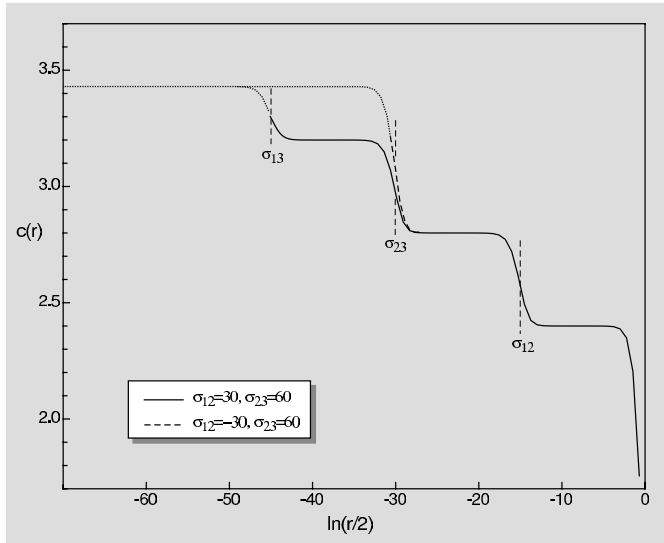


Fig. 7. The $SU(4)_3$ RG flow

4.2.6 The $Sp(4)_2$ -HSG model

Having provided some evidence for the working of the decoupling rule (3.4) at higher levels, we now want to extend this also to non-simply laced algebras, for which consistent S-matrices were proposed in [12]. Since a TBA analysis has not been carried out for the non-simply laced case, the following will also provide support for the working of the proposal in [12]. According to the latter the $Sp(4)_2$ -HSG model is comprised out of four stable particles:

$$\begin{aligned}
 \mathcal{P} = \{ & (1, 1) = \overline{(1, 1)}, (1, 2) = \overline{(3, 2)}, (2, 2) \\
 & = \overline{(2, 2)}, (3, 2) = \overline{(1, 2)} \},
 \end{aligned} \tag{4.64}$$

where, as before, we refer to every particle by two quantum numbers (a, i) . Labeling the rows and columns of the S-matrix in the same order as in (4.64) and particularizing the closed formulae provided in [12] yields

$$S_{Sp(4)_2} = \begin{pmatrix} -1 & -(\sigma_{12}, 2) & (\sigma_{12}, 1)(\sigma_{12}, 3) & -(\sigma_{12}, 2) \\ -(\sigma_{21}, 2) & i(0, -2) & -(0, -1)(0, -3) & -i(0, -2) \\ (\sigma_{21}, 1)(\sigma_{21}, 3) & -(0, -1)(0, -3) & (0, -2)^2 & -(0, -1)(0, -3) \\ -(\sigma_{21}, 2) & -i(0, -2) & -(0, -1)(0, -3) & i(0, -2) \end{pmatrix}, \tag{4.65}$$

where $\sigma_{12} = -\sigma_{21}$ is the only resonance parameter in the theory and we employed the building blocks (4.4). Carrying out the logarithmic derivative of the individual components of $S_{Sp(4)_2}$ yields the kernel

$$\begin{aligned}
 \Phi_{Sp(4)_2} = & \begin{pmatrix} 0 & \frac{1}{\cosh(\theta+\sigma_{12})} & \frac{2\sqrt{2} \cosh(\theta+\sigma_{12})}{\cosh 2(\theta+\sigma_{12})} & \frac{1}{\cosh(\theta+\sigma_{12})} \\ \frac{1}{\cosh(\theta+\sigma_{21})} & \frac{-1}{\cosh \theta} & \frac{-2\sqrt{2} \cosh \theta}{\cosh 2\theta} & \frac{-1}{\cosh \theta} \\ \frac{2\sqrt{2} \cosh(\theta+\sigma_{21})}{\cosh 2(\theta+\sigma_{21})} & \frac{-2\sqrt{2} \cosh \theta}{\cosh 2\theta} & \frac{-2}{\cosh \theta} & \frac{-2\sqrt{2} \cosh \theta}{\cosh 2\theta} \\ \frac{1}{\cosh(\theta+\sigma_{21})} & \frac{-1}{\cosh \theta} & \frac{-2\sqrt{2} \cosh \theta}{\cosh 2\theta} & \frac{-1}{\cosh \theta} \end{pmatrix}.
 \end{aligned} \tag{4.66}$$

We are content here with the presentation of the analytic approximations for the plateaus. As we are dealing with functions strongly peaked at the origin, we can approximate the TBA equations and obtain the effective central charge in the deep UV from the constant TBA equations (4.53). The N -matrix involved in there reads

$$\begin{aligned}
 N_{Sp(4)_2} &= \frac{1}{2\pi} \int_{-\infty}^{\infty} d\theta \Phi_{Sp(4)_2}(\theta) \\
 &= \begin{pmatrix} 0 & 1/2 & 1 & 1/2 \\ 1/2 & -1/2 & -1 & -1/2 \\ 1 & -1 & -1 & -1 \\ 1/2 & -1/2 & -1 & -1/2 \end{pmatrix}.
 \end{aligned} \tag{4.67}$$

One can easily check that the same matrix (4.67) is also obtained when specializing the general formula given in [12]. The corresponding constant TBA solutions of (4.53) are

$$x_1^1 = 3, \quad x_1^2 = x_1^4 = 2/3, \quad x_1^3 = 4/5, \tag{4.68}$$

which yield the Virasoro effective central charge

$$c_{\text{eff}} = \frac{6}{\pi^2} \left[\mathcal{L} \left(\frac{3}{4} \right) + 2\mathcal{L} \left(\frac{2}{5} \right) + \mathcal{L} \left(\frac{4}{9} \right) \right] = 2, \quad (4.69)$$

in complete agreement with the expectations (4.2), for $k = 2$, $\ell = 2$, $h = 4$ and $h^\vee = 3$. Let us now apply the decoupling rule to (4.65). We expect²

$$\begin{array}{ccc} \begin{array}{c} \bullet \leftarrow \bullet \\ \bullet \leftarrow \bullet \\ \bullet \leftarrow \bullet \end{array} & Sp(4)_2 & 2 \\ \rightarrow \sigma_{12} & & \\ \begin{array}{c} \bullet \quad \bullet \\ \bullet \quad \bullet \end{array} & SU(2)_2 \otimes SU(2)_4 & 1.5 \end{array}$$

Indeed taking the limit $\sigma_{12} \rightarrow \infty$ in (4.66) gives the N -matrix

$$\lim_{\sigma_{12} \rightarrow \infty} N_{Sp(4)_2} = \begin{pmatrix} 0 & 0 & 0 & 0 \\ 0 & -1/2 & -1 & -1/2 \\ 0 & -1 & -1 & -1 \\ 0 & -1/2 & -1 & -1/2 \end{pmatrix}. \quad (4.70)$$

We note that particle (1, 1) has completely decoupled from the other particles. The solutions of the constant TBA equations are then

$$x_1^1 = 1, \quad x_1^2 = x_1^4 = 1/2, \quad x_1^3 = 1/3, \quad (4.71)$$

which gives

$$c_{\text{eff}} = \frac{6}{\pi^2} \left[\mathcal{L} \left(\frac{1}{2} \right) + 2\mathcal{L} \left(\frac{1}{3} \right) + \mathcal{L} \left(\frac{1}{4} \right) \right] = 3/2, \quad (4.72)$$

in complete agreement with our expectations. Taking now m_1 or m_2 to infinity yields $SU(2)_4$ or $SU(2)_2$, respectively. This is what is predicted from the relations (3.9) in [18], which makes the proposal in [12] natural.

5 Conclusion

We have proposed a new bootstrap principle, which involves also unstable particles in the scattering processes. So far, only primary unstable particles were analyzed in the literature, which occurred merely as side products in the scattering processes of stable particles. Our proposal goes beyond this and has predictive power, as it allows one to evaluate the mass spectrum of further unstable particles, such as secondaries, tertiaries, etc. In addition, it explains the degeneracy of tertiary unstable particles and possibly of higher generations for certain theories.

We commented on the general Lie algebraic picture, which underlies the construction of all known scattering theories which involve unstable particles in their spectrum. Within this picture we propose various new scattering matrices for combinations of algebras not explored so far.

² Here the arrow in the Dynkin diagram is not related to the sign of σ and has the usual meaning, that is, pointing from the long to the short root.

Furthermore, we proposed a consistent way to go beyond scaling theories of statistical models and to incorporate an effective coupling constant. The structure of the models obtained in this way can be enhanced by a complexification of the coupling constant and hence combines the ‘‘roaming models’’ with ‘‘Lie algebraic’’ ones. A more detailed analysis of these latter models would be very interesting and lead to yet unknown staircase patterns in the RG flow.

For all integrable scattering theories which are of the general form as discussed in Sect. 3, we formulate a new Lie algebraic decoupling rule which predicts the fixed points of the RG flow from the ultraviolet to the infrared. The decoupling rule is in agreement with the bootstrap construction. Still, it would be highly desirable to derive the decoupling rule more rigorously from first principles.

Our proposals are additionally confirmed by a TBA analysis, which reproduces the bootstrap prediction of the mass spectrum of unstable particles including those which are degenerate and hence invisible in the RG flow. For the HSG models the implications are that each positive root is associated to a particle. All predictions from our decoupling rule are in perfect agreement with the outcome of our TBA analysis, even for involved high rank algebras such as E_6 , for higher level and the non-simply laced case.

Acknowledgements. O.A. C-A. and A.F. are grateful to the Deutsche Forschungsgemeinschaft (Sfb288) for financial support. J.D. is grateful to the Studienstiftung des deutschen Volkes for financial support.

References

1. B. Schroer, T.T. Truong, P. Weisz, Phys. Lett. B **63**, 422 (1976); M. Karowski, H.J. Thun, T.T. Truong, P. Weisz, Phys. Lett. B **67**, 321 (1977); A.B. Zamolodchikov, JETP Lett. **25**, 468 (1977)
2. A. Fring, R. Köberle, Nucl. Phys. B **421**, 159 (1994)
3. R. Konik, A. LeClair, Phys. Rev. B **58**, 1872 (1998)
4. O.A. Castro-Alvaredo, A. Fring, Phys. Rev. D **64**, 085005 (2001)
5. Q.-H. Park, Phys. Lett. B **328**, 329 (1994); T.J. Hollowood, J.L. Miramontes, Q.-H. Park, Nucl. Phys. B **445**, 451 (1995); C.R. Fernández-Pousa, M.V. Gallas, T.J. Hollowood, J.L. Miramontes, Nucl. Phys. B **484**, 609 (1997)
6. C. Cohen-Tannoudji, Quantum mechanics (John Wiley, New York 1977)
7. R.J. Eden, P.V. Landshoff, D.I. Olive, J.C. Polkinghorne, The analytic S-matrix (CUP, Cambridge 1966)
8. G. Breit, E.P. Wigner, Phys. Rev. **49**, 519 (1936)
9. J.E. Humphreys, Introduction to Lie algebras and representation theory (Springer, Berlin 1972)
10. J.L. Miramontes, C.R. Fernández-Pousa, Phys. Lett. B **472**, 392 (2000)
11. O.A. Castro-Alvaredo, A. Fring, C. Korff, J.L. Miramontes, Nucl. Phys. B **575**, 535 (2000)
12. C. Korff, Phys. Lett. B **501**, 289 (2001)
13. A. Fring, C. Korff, Phys. Lett. B **477**, 380 (2000)
14. A.B. Zamolodchikov, Resonance Factorized Scattering and Roaming Trajectories, Preprint ENS-LPS-335 (1991)

15. A.E. Arinshtein, V.A. Fateev, A.B. Zamolodchikov, Phys. Lett. B **87**, 389 (1979); R. Köberle, J.A. Swieca, Phys. Lett. B **86**, 209 (1979); H.W. Braden, E. Corrigan, P.E. Dorey, R. Sasaki, Nucl. Phys. B **338**, 689 (1990)
16. L. Castillejo, R.H. Dalitz, F.J. Dyson, Phys. Rev **101**, 453 (1956)
17. E.B. Dynkin, Am. Math. Soc. Trans. Ser. 2 **6**, 111 (1957)
18. A. Kuniba, Nucl. Phys. B **389**, 209 (1993)
19. P. Goddard, A. Kent, D. Olive, Phys. Lett. B **152**, 88 (1985)
20. O.A. Castro-Alvaredo, A. Fring, Phys. Rev. D **64**, 085007 (2001)
21. A.B. Zamolodchikov, Int. J. Mod. Phys. A **4**, 4235 (1989)
22. E. Witten, Commun. Math. Phys. **92**, 455 (1984); V.A. Fateev, A.B. Zamolodchikov, Sov. Phys. JETP **62**, 215 (1985); D. Gepner, Nucl. Phys. B **290**, 10 (1987); D. Gepner, Z. Qiu, Nucl. Phys. B **285**, 423 (1987)
23. S. Coleman, H.J. Thun, Commun. Math. Phys. **61**, 31 (1978)
24. A.B. Zamolodchikov, Nucl. Phys. B **342**, 695 (1990); B **358**, 497 (1991); B **366**, 122 (1991)
25. J. Dreißig, Non-Perturbative Identification of New Unstable Particles in the Homogeneous Sine-Gordon Model, Diploma Thesis, Freie Universität Berlin, August 2002
26. J.L. Miramontes, talk presented at the Workshop on Integrable Theories, Solitons and Duality (São Paulo, IFT, July 2002)